Title: The Evolutionary History of Small RNAs in the Solanaceae

Short Title: Solanaceae Small RNA Evolution

Patricia Baldrich[1,*], Sébastien Bélanger[1,*], Shuyao Kong[2,*], Suresh Pokhrel[1,2,*], Saleh Tamim[4,5,*], Chong Teng[1], Courtney Schiebout[1,6], Sai Guna Ranjan Gurazada[4,7], Pallavi Gupta[1,8], Parth Patel[4,9], Mayumi Nakano[1], Ayush Dusia[4,10], Blake C. Meyers[1,3,#], and Margaret H. Frank[1,2,#]

* Contributed equally to the work (in alphabetical order)

#co-corresponding authors: Blake Meyers (bmeyers@danforthcenter.org) and Margaret Frank (mhf47@cornell.edu)

1 - Donald Danforth Plant Science Center, St. Louis, MO 63132

2 - School of Integrative Plant Science, Cornell University, Ithaca, NY 14853

3 - Division of Plant Sciences, University of Missouri, Columbia, MO 65211

4 - Center for Bioinformatics and Computational Biology, University of Delaware, Newark DE 19711

5 - Current address: Genomics Research Center, AbbVie, North Chicago IL 60064

6 - Current address: Dartmouth College

7 - Corteva Agriscience, Wilmington, DE 19805

8 - Institute for Data Science & Informatics, University of Missouri, Columbia, MO 65211

9 - Current address: Johnson & Johnson

10 - Current address: VMware Inc.

Margaret H. Frank, Donald Danforth Plant Science Center, St. Louis, MO 63132; Current: Cornell University, School of Integrative Plant Science, Ithaca, NY 14853 https://orcid.org/0000-0002-8269-8240

*Sébastien Bélanger, Donald Danforth Plant Science Center, St. Louis, MO 63132 https://orcid.org/0000-0002-6755-8207

*Saleh Tamim, Center for Bioinformatics and Computational Biology, University of Delaware, Newark DE 19711, Current: Genomics Research Center, AbbVie, North Chicago IL 60064. http://orcid.org/0000-0002-6215-7041

Chong Teng, Donald Danforth Plant Science Center, St. Louis, MO 63132 https://orcid.org/0000-0001-9898-6442

*Patricia Baldrich, Donald Danforth Plant Science Center, St. Louis, MO 63132 https://orcid.org/0000-0003-4669-6632

*Suresh Pokhrel, Division of Plant Sciences, University of Missouri, Columbia, MO 65211; Donald Danforth Plant Science Center, St. Louis, MO 63132 http://orcid.org/0000-0002-5323-1940

Blake C. Meyers, Division of Plant Sciences, University of Missouri, Columbia, MO 65211; Donald Danforth Plant Science Center, St. Louis, MO 63132 https://orcid.org/0000-0003-3436-6097

*Shuyao Kong, Cornell University, School of Integrative Plant Science, Ithaca, NY 14853 https://orcid.org/0000-0002-3124-8899

Previous contributors:

Mayumi Nakano, Donald Danforth Plant Science Center, St. Louis, MO 63132 https://orcid.org/0000-0001-9317-4509

Ayush Dusia, University of Delaware, Newark DE 19711. current: VMware Inc., https://orcid.org/0000-0003-1310-8523

Pallavi Gupta, Institute for Data Science & Informatics, University of Missouri, Columbia, MO 65211. https://orcid.org/0000-0003-0146-239X

Courtney Schiebout, Donald Danforth Plant Science Center, current: Dartmouth College, https://orcid.org/0000-0002-4830-8237

Parth Patel, Center for Bioinformatics and Computational Biology, University of Delaware, Newark DE 19711, current: Johnson & Johnson, https://orcid.org/0000-0002-0195-3933

Sai Guna Ranjan Gurazada, Center for Bioinformatics and Computational Biology, University of Delaware, Newark DE 19711, Current: Corteva Agriscience, Wilmington, DE 19805. https://orcid.org/0000-0002-3084-5683

ONE-SENTENCE SUMMARY

We use over 255 publicly-available small RNA datasets to characterize the small RNA landscape for the Solanaceae family.

AUTHOR CONTRIBUTIONS

B.C.M and M.H.F. conceived the original research plan and supervised the analyses, and supervised and completed the writing; P.B., S.B., S.K., S.P., S.T., C.T., C.S., S.G.R.G, P. G. and P.P. performed the analyses, generated tables and figures, and contributed to writing of the article; M.N and A.D. provided technical assistance with data processing. M.H.F. agrees to serve as the author responsible for contact and ensures communication.

FUNDING INFORMATION

The work was supported with funding from NSF IOS awards 1842698, 754097 and 1650843, and USDA NIFA award 2019-67013-29010 to Meyers; NSF award 1523668 to M. Frank.

ABSTRACT

The Solanaceae or “nightshade" family is an economically important group that harbors a remarkable amount of diversity. To gain a better understanding of how the unique biology of the Solanaceae relates to the family’s small RNA genomic landscape, we downloaded over 255 publicly available small RNA datasets that comprise over 2.6 billion reads of sequence data. We applied a suite of computational tools to predict and annotate two major small RNA classes: (1) microRNAs (miRNAs), typically 20-22 nt RNAs generated from a hairpin precursor and functioning in gene silencing, and (2) short interfering RNAs (siRNAs), including 24-nt heterochromatic siRNAs (hc-siRNAs) typically functioning to repress repetitive regions of the genome via RNA-directed DNA methylation, as well as secondary phased siRNAs (phasiRNAs) and trans-acting siRNAs (tasiRNAs) generated via miRNA-directed cleavage of a Pol II-derived RNA precursor. Our analyses described thousands of small RNA loci, including poorly-understood clusters of 22-nt siRNAs that accumulate during viral infection. The birth, death, expansion, and contraction of these small RNA loci are dynamic evolutionary processes that characterize the Solanaceae family. These analyses indicate that individuals within the same genus share similar small RNA landscapes, whereas comparisons between distinct genera within the Solanaceae reveal relatively few commonalities.

117

118 **INTRODUCTION**

119

120 Plant genomes encode thousands of small RNA (sRNA) loci that participate in a wide
121 variety of processes, including developmental transitions, epigenetic patterning, biotic
122 and abiotic stress responses, and local and long-distance communication. sRNAs are
123 18 to 24 nucleotide (nt) non-coding sequences that are loaded into Argonaute (AGO)
124 proteins to direct transcriptional or post-transcriptional gene silencing in a sequence-
125 specific manner. sRNAs can be divided into different classes based on their length,
126 biogenesis, and mode of action. This study focuses on microRNAs (miRNAs) and short
127 interfering RNAs (siRNAs).

128 MicroRNAs are typically 21- or 22-nt in length and originate from a self-complementary,
129 single-stranded (ss)RNA molecule, a Pol II product, that forms a hairpin structure. This
130 characteristic secondary structure is typically recognized by DICER-LIKE 1 (DCL1) and
131 processed through two sequential cleavage events into a mature double-stranded
132 (ds)RNA duplex; each of these mature miRNAs has the potential to be loaded into
133 Argonaute effector proteins (Axtell et al., 2011).

134 Small interfering RNAs (siRNAs) can be divided into multiple categories: hairpin
135 siRNAs, which are generated in a manner similar to miRNAs, heterochromatic siRNAs
136 (hc-siRNAs), and secondary siRNAs. hc-siRNAs are the most abundant and diverse
137 sRNA class in plants; they are typically 24-nt in length and originate from
138 heterochromatic regions of the genome (e.g. repetitive regions and transposable
139 elements). hc-siRNA precursors are transcribed by RNA Pol IV, converted into dsRNA
140 by RNA-DEPENDENT RNA POLYMERASE 2 (RDR2), and finally recognized and
141 cleaved by DCL3, generating mature duplexes of which individual sRNAs guide
142 sequence-specific RNA-directed DNA methylation (RdDM) (Won et al., 2014). In
143 contrast, secondary siRNAs are generated from coding and non-coding Pol II transcripts
144 and require a miRNA “trigger” to initiate production. Secondary siRNAs include phased
145 siRNAs (phasiRNAs), trans-acting siRNAs (tasiRNAs), and epigenetically activated
146 siRNAs (easiRNAs). PhasiRNA production is typically initiated by a 22-nt miRNA trigger

147 that recognizes and directs the cleavage of ssRNA targets, which are then transformed
148 into dsRNA by RDR6, and processed into “in phase” sRNAs via cleavage in a
149 sequential manner by DCL4 and DCL5 (Fei et al., 2013; Chen et al., 2018b).

150 The evolutionary history of sRNA biogenesis pathways is complex. While the core
151 pathways supporting the biogenesis of major sRNA classes are conserved across the
152 land plants, lineage-specific instances of duplication, subfunctionalization, and gene
153 loss often lead to complicated evolutionary relationships amongst AGO, DCL, and RDR
154 family members. In the AGO family, the moss genome of *Physcomitrella patens*, for
155 instance, contain three *AGO* genes (AGO1/4/7), while flowering plant genomes often
156 contain 10 to 20 *AGO* family members (Axtell, 2018). The Arabidopsis genome, for
157 example, contains ten *AGO* genes encoding proteins that can be broadly grouped into
158 three clades: AGO1/5/10, AGO2/3/7/8, and AGO4/6/9 (Zhang et al., 2015). These
159 individual AGO clades interact with distinct classes of sRNAs. For example, AGO1
160 predominantly binds 21 or 22-nt miRNAs, AGO4 binds 24-nt hc-siRNAs in the canonical
161 RNA dependent DNA methylation (RdDM) pathway, while AGO2 binds 22-nt siRNAs
162 that function in viral responses (Ma and Zhang, 2018). Additional AGOs have
163 undergone further subfunctionalization in select species, for example, there are four
164 AGO1 paralogs in rice, each of which has distinct miRNA binding affinities (Wu et al.,
165 2009). There are also instances of *de novo* function arising within the AGO gene family.
166 For example, maize AGO18b is a grass-specific AGO that functions the regulation of
167 inflorescence meristem development and negatively regulates spikelet number on the
168 tassel (Sun et al., 2018). Despite the functional importance of gene family expansion
169 and contraction amongst key components of sRNA biogenesis machinery, relatively
170 little characterization of the DCL, RDR, and AGO families has been carried out in the
171 Solanaceae. Existing data focused on small subsets of Solanaceae species have
172 uncovered lineage-specific expansion events within the AGO (Liao et al., 2020), RDR,
173 and DCL families (Esposito et al., 2018). Given the abundance of genomic resources
174 now available for the Solanaceae, a more comprehensive, cross-species
175 characterization of these gene family members will help resolve questions with respect
176 to the evolution of unique aspects of sRNA biogenesis within this family.

The Solanaceae harbors a remarkable amount of morphological and metabolomic diversity. The nightshade family includes staple crops (e.g. potato and eggplant), high-value crops (e.g. tomato, pepper, petunia, and tobacco), and emerging crop systems (e.g. ground cherry), making it the third most economically important plant family in the world. Moreover, several species in the Solanaceae family serve as popular model systems for studies of biological processes pronounced within this family, including fruit ripening (Klee and Giovannoni, 2011; Shinozaki et al., 2018), plant-pathogen interactions (Goodin et al., 2015; Pombo et al., 2020), and the production of specialized metabolites (Fan et al., 2019; Leong et al., 2019). These model systems are supported by high-quality reference genomes (Mueller et al., 2005; Potato Genome Sequencing Consortium et al., 2011; Bombarely et al., 2012; Tomato Genome Consortium, 2012; Qin et al., 2014; Bombarely et al., 2016) that have facilitated the generation and analysis of genomic-scale deep sequencing datasets within the family. There are currently more than 250 Solanaceae libraries, equating to over 2.6 billion reads of publicly-available sRNA data available in the NCBI short read archive (SRA). Previous work focused on specific aspects of sRNA biology within the Solanaceae have identified unique sRNA phenomena that are associated with the diverse biology of this family. One specific case is the miR482/miR2118 superfamily in Solanaceae, which also includes miR5300 members. In eudicots, this family of 22-nt miRNAs targets the encoded sequence of the P-loop motif of NLR disease resistance proteins (Shivaprasad et al., 2012), generating a secondary siRNA cascade with implications for basal innate immunity (Zhai et al., 2011; Shivaprasad et al., 2012). Evolutionary studies indicate that this superfamily originated prior to the split of the Solanum and *Nicotiana* genera (de Vries et al., 2015), and superfamily members have even been found in Gymnosperm species, indicating that this miRNA family has deep evolutionary origins (Xia et al., 2015).

Genomic resources that support cross-species analyses in land plants have grown substantially over the last two decades. There are now more than 200 fully-sequenced genomes covering major branches of the land plant phylogeny. In addition to the availability of plant genomes, innovations in RNA library construction and sequencing technologies, as well as algorithms and bioinformatic resources, have drastically

208 reduced experimental costs and facilitated the large-scale production of publicly-
209 available sRNA sequence data. Two recent studies using publicly-available and newly
210 generated sRNA datasets harvested from a broad range of land plant taxa have taken
211 advantage of these resources and substantially improved the annotation of miRNA,
212 phasiRNA and hc-siRNA loci in land plant genomes (Lunardon et al., 2020; Chen et al.,
213 2019). These studies both show that siRNA loci are minimally conserved across
214 species, while mature miRNAs tend to be conserved across lineages (Chen et al., 2019;
215 Lunardon et al., 2020). There are numerous lineages- or species-specific miRNA
216 sequences which correspond to young miRNAs (Cuperus et al., 2011; Chávez Montes
217 et al., 2014; Lunardon et al., 2020). Although large-scale studies produce a massive
218 amount of data and describe major evolutionary trends, they are often unable to capture
219 lineage- and species-specific phenomena.

220 In this study, we applied a suite of computational tools to a large collection of publicly-
221 available sRNA libraries to investigate the unique aspects of miRNAs and siRNA
222 biology within the Solanaceae. We describe thousands of sRNA loci, some of which are
223 unique to the Solanaceae. For example, we found that an annotated, Solanaceae-
224 specific miRNA family is actually a MITE-derived siRNA, and we observed family-wide
225 expression of *DCL2*-derived 21-nt phasiRNAs. Our analyses also revealed aspects of
226 sRNA biology that are only conserved at the sub-family level, including a lineage-
227 specific expansion of previously unidentified miRNAs in *Nicotiana*, a distinct split in
228 phasiRNA production between the *Solanum*/*Capsicum* and *Nicotiana*/*Petunia* branches
229 of the family, and distinct clusters of 22-nt sRNAs that are expressed in response to
230 viral infection in tomato. Overall, our analyses indicate that individuals within the same
231 genus share similar sRNA landscapes, whereas comparisons between distinct genera
232 within the Solanaceae reveal relatively few commonalities.
233

234 **MATERIALS AND METHODS**

235

236 **Evolution of small RNA biogenesis protein genes in the Solanaceae**

We downloaded protein sequence files from Phytozome v13, the Sweetpotato Genomics Resource, and the SOL Genomics Network databases, and selected proteomes for *Arabidopsis thaliana*, two Convolvulaceae (*Ipomoea trifida* and *Ipomoea triloba*) and the seven Solanaceae species (*Nicotiana benthamiana*, *Nicotiana tabacum*, *Petunia axillaris*, *Petunia inflata*, *Capsicum annuum*, *Solanum lycopersicum* and *Solanum tuberosum*) for analysis (Supplemental Table 1). We used SonicParanoid v1.2.6 (Cosentino and Iwasaki, 2018) and OrthoFinder v2.3.11 (Emms and Kelly, 2015) to perform a gene orthology inference using default parameters. To identify orthologous groups related to NRP, RDR, DCL, DRB and AGO proteins, we used the reference protein IDs available in the UniProt database for *A. thaliana*. We then aligned the retrieved protein sequences using default parameters in MUSCLE v3.8.1551 (Edgar, 2004), and trimmed alignments with trimAL v1.4.rev15 applying the -gappyout option (Capella-Gutierrez et al., 2009). To infer phylogenetic trees we implemented the maximum likelihood method in IQ-TREE v1.6.12 with the following parameters: -alrt 1000 and -bb 1000 (Minh et al., 2013; Nguyen et al., 2015; Kalyaanamoorthy et al., 2017). We used iTOL v4 (Letunic and Bork, 2019) to visualize consensus trees and summarize orthologous protein genes for the five gene families investigated in each species (Supplemental Table 1). To investigate organ-specific expression for the DCL1, AGO1, and AGO2 paralogs identified for tomato, we downloaded expression data for *Solanum lycopersicum* from The Bio-Analytic Resource for Plant Biology (Waese et al., 2017).

Data collection, quality filters, and read processing

We downloaded raw sRNA seq and PARE libraries for *Solanum lycopersicum* (tomato), *S. tuberosum* (potato), *Nicotiana benthamiana*, *N. tabaccum* (tobacco), *Capsicum annum* (pepper), *Petunia axillaris/P. inflata* (petunia) from the NCBI SRA (https://www.ncbi.nlm.nih.gov/sra; detailed information regarding raw and processed libraries can be found in Supplemental Dataset 1. Briefly, we processed raw FASTQ reads using a Python script that performs quality filtering, trimming, adapter removal, and then converts reads into chopped tag count files (https://github.com/atulkakrana/preprocess.seq (Bolger et al., 2014)). We then mapped our reads to their respective reference genomes (Table 1) using Bowtie 1 (Langmead,

2010) allowing for zero mismatches. We applied two criteria for filtering out low-quality data: first, we excluded libraries with low mapping rates, and second, we removed libraries that lacked a significant accumulation of 21-nt and 24-nt reads based on size distribution plots (Supplemental Figure 1), indicating potential RNA degradation. We assembled species-specific expression databases using these final, high-quality, processed datasets (Nakano et al., 2020).

Solanaceae genome versions and functional gene annotations

We used the following reference genomes and their associated annotation files to build expression databases and perform the bioinformatic analyses described in this study: *Capsicum annum* Zunla-1 v2.0 (http://public.genomics.org.cn/BGI/pepper/) (Qin et al., 2014), *Petunia axillaris* and *P. inflata* (Bombarely et al., 2016), *Nicotiana tabacum* v4 (Edwards et al., 2017), *Nicotiana benthamiana* v 0.3 (Bombarely et al., 2012), *Solanum tuberosum* (Potato Genome Sequencing Consortium, 2011), and *Solanum lycopersicum* build 2.5 (Tomato Genome Consortium, 2012) (ftp://ftp.solgenomics.net/genomes/).

MicroRNA Predictions

We used three different software packages to obtain a robust prediction of microRNAs (miRNAs) across our Solanaceous model genomes: ShortStack (Axtell, 2013), miR-PREFeR (Lei and Sun, 2014), and miRPD (a version of miReap optimized for plant miRNA prediction; (Sun et al., 2013)). We standardized the minimum mapping coverage and size of hits across the three programs in order to control for dissimilarities in software performance.The vast majority of miRNAs fall between 20-22 nt in length so we narrowed our predictions to this 20-22 nt size range. Each program employs a different method for calculating coverage. In ShortStack we set the minimum coverage to 15, while in miR-PREFeR and miRPD we set the minimum coverage to 20. We then filtered out predicted miRNA precursors based on recently published guidelines for miRNA predictions (Axtell and Meyers, 2018). Briefly, we required that all miRNAs express both strands of the miRNA duplex (the mature miRNA and miRNA-star), and originate from a precursor that folds with a normalized minimum free energy (MFE) of < -0.2 kcal/mol/nucleotide. Notably, enforcing the expression of a complementary miRNA-

299 star sequence resulted in little to no filtering, so we applied a more stringent filter
300 requiring that the abundance of the complementary miRNA-star reads were ≥10% of the
301 abundance of the mature miRNA.
302
303 We applied additional filtering for "novel" miRNAs that did not match miRBase entries
304 (see "miRNA conservation across species," below). To remove hairpin structures that
305 might originate from MITEs and tRNAs, we filtered out novel miRNAs that aligned to our
306 list of annotated transposable elements (TEs) and tRNA datasets for the Solanaceae
307 (Supplemental Dataset 2). We found a surprising number of novel miRNAs in our
308 *Nicotiana benthamiana* (hereafter, "benthi") dataset which warranted manual curation.
309 To investigate whether our novel benthi miRNAs originate from conanonical precursor
310 structures, we mapped our shortread data onto predicted miRNA precursors using
311 structVis v0.4 (github: https://github.com/MikeAxtell/strucVis), and removed novel
312 miRNAs that showed non-canonical folding and/or miRNA/miRNA* expression. After
313 these filtering steps we found the miRPD results to be highly inconsistent, producing
314 unrealistically high numbers of predicted miRNAs for some of our species and zero
315 predicted miRNAs for others. Thus, we decided to limit our analyses to the ShortStack
316 and miR-PREFeR results. To create a consensus set of miRNAs for these two
317 prediction programs, we collapsed precursors with overlapping coordinates from these
318 two software programs into unique entries. Overall, we found that ShortStack was more
319 conservative, predicting fewer miRNAs than miR-PREFeR; however, the miRNAs were
320 also predicted with appreciable confidence and resulted in minimal post-prediction
321 filtering. Our hybrid prediction approach in combination with stringent filtering allowed
322 for sensitive, yet robust predictions across the species.
323
324 **MicroRNA conservation across species**
325 To facilitate cross species comparisons of conserved and novel miRNAs within the
326 Solanaceae, we first clustered mature miRNA sequences for the predicted miRNAs
327 (described above) into families by requiring pairwise sequence overlap of ≥ 75%. To
328 annotate the miRNA families, we aligned mature miRNA sequences to the latest v22

329 miRBase database of all land plants requiring an 85% match, and provided new IDs for
330 novel miRNA families (Kozomara and Griffiths-Jones, 2014; Kozomara et al., 2019). We
331 tabulated all novel and previously annotated miRNA families across the Solanaceae in a
332 master table that reports presence and absence for each miRNA family (Supplemental
333 Dataset 3).
334
335 **_PHAS_ locus predictions and annotations**
336 We used three programs to identify *PHAS* loci: ShortStack (Axtell, 2013), PHASIS
337 (Kakrana et al., 2017), and PhaseTank (Guo et al., 2015). We ran PHASIS and
338 PhaseTank using the default parameters listed in the program manuals and filtered the
339 results for high-confidence loci that were identified with a p-value of ≤.001. We ran
340 ShortStack using the same parameters that were applied to our miRNA predictions.
341 PhaseTank did not perform consistently across the analyzed genomes; it only reported
342 *PHAS* loci for unassembled regions of the genomes. After we removed unassembled
343 contigs, the program returned no results, so we decided to remove PhaseTank from our
344 analysis pipeline. We merged the *PHAS* loci obtained from PHASIS and ShortStack into
345 a single list for each species, and collapsed loci located within 400 nucleotides of each
346 other into individual *PHAS* predictions (Supplemental Dataset 4).
347
348 We annotated coding versus non-coding *PHAS* loci using available CDS GFF files. To
349 characterize non-coding *PHAS* loci we aligned our non-coding *PHAS* loci to the NCBI
350 non-redundant (nr) database and annotated the loci with one of the top ten hits using
351 default alignment parameters in BLAST (Altschul et al., 1990). To test whether coding
352 *PHAS* loci were generated from orthologous genes across species, we constructed
353 gene orthogroups for species with associated peptide fasta files. Finally, we linked
354 these orthogroup predictions with annotation files for tomato, Arabidopsis, and pepper
355 (Supplemental Dataset 5). The published pepper gff file lacks annotations, so we
356 generated our own pepper annotation file by running a BLASTP search against the
357 NCBI NR database and retrieving the best BLAST hit for each entry.
358
359 **miRNA target predictions**

360 We used sPARTA, a miRNA target prediction program to identify miRNA targets with
361 the following specifications: -genomeFeature 0 -tarPred H -tarScore S (Kakrana et al.,
362 2015). We applied a cut off score of ≥ 4 to filter for reliable miRNA-target interactions.
363 *PHAS* loci are triggered by 22 bp miRNAs that have a 5' Uracil bias (Chen et al., 2010;
364 Cuperus et al., 2010). We ran sPARTA with the -featureFile option to identify miRNAs
365 from our predicted miRNA list that trigger *PHAS* locus production from our predicted
366 PhasiRNA list. We applied a quality score of ≥ 4 to filter for PHAS locus triggers,
367 prioritized miRNA triggers that start with Uracil (U), and selected miRNA triggers equal
368 to 22 bp with the exception of miR390.
369
370 **hc-siRNAs and transposable elements across SOL genomes**
371 To analyze hc-siRNAs, we first ran RepeatMasker (http://www.repeatmasker.org) on
372 each one of the analyzed genomes using the Viridiplantae RepBase database
373 (http://www.girinst.org/repbase) as a library, to identify transposable elements (TE).
374 Next, we used the identified TEs as a database to map sRNA reads using Bowtie
375 (Langmead, 2010) with default parameters and categorized all 24-nt long reads that
376 mapped to any of our identified TEs as hc-siRNAs. It was impossible to identify the
377 specific origin of these sRNAs due to the repetitive nature of TEs, so we only
378 considered TE superfamilies for this study. Genome-wide representation of hc-siRNAs
379 was visualized by plotting Manhattan plots with the qqman R package (Turner, 2014).
380 We plotted the data based on the genome mapping coordinate along the chromosome
381 for each hc-siRNA and its relative abundance.
382
383 **Identification of 22-nt clusters expressed in response to Geminivirus infection**
384 To discover 22-nt sRNA clusters that may be linked to Geminivirus infection in tomato,
385 we downloaded sRNA libraries for control and infected treatments from the
386 TOMATO_sRNA_SOL Next-Gen DB (Nakako et al., 2020) and filtered for 22-nt reads.
387 We tuned the parameters for 22-nt cluster identification using two fruit peel libraries
388 (Tomato_S_7 and Tomato_S_8, cv. Ailsa Craig, Gao et al., 2015) and two leaf libraries
389 (Tomato_S_50, cv. Moneymaker, and Tomato_S_53, line FL505, Bai et al., 2016). To

390 identify clusters that accumulate in response to Geminivirus infection, we analyzed two
391 infected leaf libraries (Sly_leaves_t2, cv. Pusa Ruby, Saraf et al., 2015; Tomato_S_52,
392 cv. Moneymaker, Bai et al., 2016) and their corresponding control libraries
393 (Sly_leaves_t1 and Tomato_S_50, respectively). We applied the following analysis
394 pipeline to identify 22-nt sRNA clusters: first, we ran ShortStack with the parameters
395 tuned to yield the highest reproducibility between repeated runs, relatively high similarity
396 between results from similar samples (e.g. leaf vs. leaf), and relatively high difference
397 between results from distinct samples (e.g. leaf vs. fruit peel), without compromising the
398 alignment rate (Johnson et al., 2016). This fine tuning resulted in the following
399 parameter set: --mmap u --mismatch 1 --bowtie_m 3 --ranmax 2 --pad 125 --mincov
400 75rpm. Using these parameters, we ran ShortStack to identify all of the 22-nt sRNA
401 clusters in the aforementioned four libraries. Next, we filtered out clusters that were
402 shorter than 200 bp in length, and clusters that were inconsistently expressed in one
403 infected-control sample pair, but not in the other. We applied a threshold of absolute
404 log2 fold change greater than two in order to identify differentially expressed clusters
405 between the Geminivirus infected and mock-treated samples.
406
407 **Data visualization and representation**
408 We visualized the 22-nt sRNA clusters using the transcriptome browser function in the
409 TOMATO_sRNA_SOL Expression database (Nakano et al., 2006; Nakano et al., 2020;
410 https://mpss.meyerslab.org/). We generated dot plots using the ggplot2 package
411 (Wickham, 2016), heatmaps using gplots package (Warnes et al., 2019), and heatmaps
412 of DCL2 and AGO1 paralog expression using the TBTools heatmap function (Chen et
413 al., 2018a).
414
415

RESULTS

Evolution of small RNA biogenesis genes in the Solanaceae

sRNA biogenesis and function are regulated by proteins in the Nuclear RNA Polymerase (NRP), RNA-dependent RNA polymerase (RDR), Double-stranded RNA binding protein (DRB), Dicer-Like protein (DCL) and Argonaute protein (AGO) families. To describe and interpret sRNA biogenesis and function in the Solanaceae, we performed a phylogenetic analysis of these proteins encoded in genomes of *Arabidopsis thaliana*, two Convolvulaceae outgroups (*Ipomoea trifida* and *Ipomoea triloba*) and seven Solanaceae species (*Nicotiana benthamiana*, *N. tabacum*, *Petunia axillaris*, *P. inflata*, *Capsicum annuum*, *Solanum lycopersicum* and *S. tuberosum*). In Table 2 we summarize the number of protein genes encoded for *NRP*, *RDR*, *DCL*, *DRB* and *AGO* gene families in each species. Two observations emerged from this table. First, some gene families expanded when comparing Arabidopsis to members of the Convolvulaceae and/or Solanaceae families. For instance, the number of genes expanded in the AGO family comparing *A. thaliana* (10 *AGOs*) to Convolvulaceae (13 *AGOs*) or Solanaceae for the genus *Petunia* (12 or 13 *AGOs*) and the genus *Solanum* (13 or 15 *AGOs*). A second observation was the appearance of missing gene annotations for specific gene families in certain species (e.g. *NRP* genes encoded in tomato and potato). Thus, we chose to focus on *AGO* and *DCL* gene families in all species. All annotated genes are detailed in Supplemental Table 1. Their evolutionary relationships are visualized in Figure 1 and Supplemental Figure 2.

AGO proteins are required to load sRNAs and to catalyze their functional activity. AGO proteins can either trigger the biogenesis of sRNAs, through the miRNA-directed cleavage of *TAS*/*PHAS* transcripts, or catalyze sRNA regulatory activity through transcriptional or post-transcriptional regulation. Our phylogenetic analysis identified an expansion of specific and distinct *AGO* genes for Convolvulaceae and Solanaceae species when compared to *Arabidopsis*. For example, we identified a Convolvulaceae-specific expansion for *AGO5* (to three copies) and *AGO7* (to two copies) that did not occur in the Solanaceae (Figure 1; Table 2). We also identified differential *AGO* gene

family expansion and loss across the Solanaceae. For instance, we expected to find two copies of *AGO2/AGO3* (based on gene family membership in *A. thaliana*) but we only identified one homolog in *Capsicum*, *Nicotiana ssp.* and *Petunia ssp.,* and three in *Solanum ssp.* (Figure 1; Table 2). A common feature that we observed across the Solanaceae was a family-wide expansion of *AGO1*; depending on the particular species, we identified two to three *AGO1* paralogs within the Solanaceae (Figure 1; Table 2). To test whether this *AGO1* expansion coincides with evidence for subfunctionalization, we downloaded and visualized public expression data for the two *AGO1* paralogs we identified in *Solanum lycopersicum* (Figure 1B; http://bar.utoronto.ca/eplant_tomato/). Interestingly, we observed a distinct expression pattern of both copies with one mainly accumulating during vegetative development (Solyc06g072300), while the other mainly accumulated in fruits during reproductive development (Solyc03g098280). This observation suggests that indeed, these *AGO1* paralogs are in the process of subfunctionalization in tomato. We also discovered that *AGO2* expanded into triplicate copies that are located in tandem on chromosome 2 in tomato (Figure 1A). Existing public data indicates that only one of the three *AGO2* copies is expressed, and this is predominantly during fruit development (Figure 1C). In brief, we discovered lineage-specific expansions of *AGO* subfamily members in the Convolvulaceae and Solanaceae. Public expression data for tomato indicates that these *AGO1* and *AGO2* paralogs may have subfunctionalized following duplication.

We annotated additional sRNA biogenesis genes, including *NRP*, *RDR*, *DRB* and *DCL* (Figure 2; Supplementary Figure 2; Supplementary Table 2), and discovered a subfamily expansion of *DCL2* in the *Solanum* (tomato and potato) and *Capsicum* (pepper) branch of the Solanaceae. For all three species, *DCL2* expanded through a tandem duplication on chromosome 11 (annotated as chromosome 12 for pepper). In tomato, *DCL2* underwent additional duplication events, expanding to three tandem duplicates on chromosome 11 and additional copy on chromosome 6 (Figure 2). To gain insights into the impact of gene expansion on function, we downloaded public expression data for tomato, and found that the *DCL2* copy on chromosome 6 (Solyc06g048960) is broadly throughout the whole plant and the three paralogs on chromosome 11 (Solyc11g008520; Solyc11g008530; Solyc11g008540) are specifically

enriched in flowers and fruits (Figure 2B). We also observed much higher expression levels for two of the *DCL2* paralogs on chromosome 11 (Solyc11g008530; Solyc11g008540) relative to the broadly expressed copy of *DCL2* on chromosome 6 (Solyc06g048960). Together, these observations highlight a Solanaceae-specific expansion and putative subfunctionalization of *DCL2*.

Mining publicly-available sRNA data for the Solanaceae

We selected seven core species in the Solanaceae (tomato, potato, pepper, 'petunia_ax' *Petunia axilaris*, 'petunia_in' *P. inflata*, tobacco, 'benthi' [*Nicotiana benthamiana*]) for our cross-species analyses of sRNA loci. These species were selected based on the availability of fully sequenced genome assemblies and publicly-available sRNA data. Notably, we excluded eggplant from this study due to the paucity of publicly-available *S. melongena* sequence data. In total, we analyzed over 2.6 billion sRNA reads from 255 different libraries. By far, tomato and potato were the most extensively sampled, having 84 and 73 high-quality publicly available libraries, respectively, while tobacco was the least sampled species (represented by only 9 libraries on the NCBI SRA; Supplemental Dataset 1). The depth of sequencing also varied quite substantially across libraries. This was largely due to the differences in sequencing technologies. In line with previous studies, we counterbalanced this heterogeneity in sequence depth by merging all high-quality libraries together and treating them as independent reference sets (Lunardon et al., 2020). Most of these reference sets included organ atlas samples that represent expression patterns from diverse organ systems and developmental stages. The total number of genome aligned reads for each species varied from just over 70-million reads for *Petunia axillaris* and tobacco to more than 650 million reads for tomato (Supplemental Dataset 1).

MicroRNA predictions indicate an expansion of novel miRNAs in *Nicotiana* species

We identified previously annotated and novel miRNAs across the Solanaceae using two software programs: ShortStack and miR-PREFeR (Axtell, 2013; Lei and Sun, 2014). After filtering for high-quality predictions based on hairpin folding and the presence of

508 both strands of the microRNA duplex (Axtell and Meyers, 2018), we created a
509 consensus set of miRNAs with assigned annotations based on ≥ 85% sequence
510 similarity to miRBase v22 (Supplemental Dataset 3). Overall, our analyses predicted
511 between 124 and 440 miRNAs across the Solanaceous species (Figure 3;
512 Supplemental Dataset 3). The depth of sequence data did not correlate strongly with the
513 number of miRNAs that we predicted for a given species. For example, pepper (330)
514 and benthi (440) had the highest number of predicted miRNAs by far, even though
515 these species are only supported by a moderate
516 depth of sequence data relative to tomato, which only had 194 predicted miRNAs
517 (Supplemental Dataset 3). This indicates that our miRNA predictions were generally not
518 constrained by sampling.
519
520 We were surprised to find more than 400 predicted miRNAs in the benthi genome. To
521 gain higher confidence in these benthi predictions, we manually filtered the benthi
522 miRNA precursors based on the folding and expression of their predicted precursors
523 using SructVis (Supplemental Datasets 3 & 6; https://github.com/MikeAxtell/strucVis).
524 Even after manually filtering, we had a substantial number of predicted miRNAs for
525 benthi (368), indicating that these predictions reflect a real lineage-specific miRNA
526 expansion in *Nicotiana* (Figure 3A). In agreement with this conclusion, we also identified
527 a relatively high number of miRNAs in tobacco (194), despite having the lowest depth of
528 sequence data for this species. Notably, less than half of the miRNAs that we identified
529 in either of the two *Nicotiana* genomes could be annotated using miRBase, indicating
530 that miRNA expansion in *Nicotiana* was likely driven by the evolution of "young" lineage-
531 specific miRNAs.
532
533 We also uncovered a substantial expansion of predicted miRNAs in pepper (330), which
534 is congruent with previous miRNA predictions for this species (Seo et al., 2018; Taller et
535 al., 2018). In contrast, we predicted relatively few miRNAs for both of the petunia
536 genomes (124 - *P. inflata* and 126 - *P. axillaris*). This reduced number of predicted
537 miRNAs in petunia may simply reflect a lack of sample diversity for these species;
538 publicly-available sRNA-seq datasets for petunia are predominantly composed of floral

539 samples (Supplemental Dataset 1). Indeed, a previous analysis using combined miRNA
540 prediction software and a homology based search for known miRNAs uncovered about
541 140 miRNAs for both petunia genomes, indicating that our *de novo* predictions on their
542 own are missing putative miRNA loci. Increasing the diversity of sRNA samples would
543 likely improve miRNA annotations for this genus (Bombarely et al., 2016). Finally, we
544 only identified a moderate number of predicted miRNAs in the Solanum genus (potato =
545 160, tomato = 194), despite having a substantial amount of sequence data (>80 sRNA
546 libraries) for tomato. Solanum is by far the best characterized genus in the Solanaceae
547 with regard to sRNA biology. Given that our predictions for this genus are similar to
548 those from previous studies, we are likely approaching saturation for Solanum-specific
549 miRNA predictions (Tomato Genome Consortium, 2012; Zhang et al., 2013; Cardoso et
550 al., 2018; Zuo et al., 2020; Deng et al., 2021).
551
552 **miRNA families are conserved within genera**
553 To gain insight into miRNA conservation across Solanaceous species, we collapsed all
554 predicted miRNAs into clusters using a 75% sequence similarity cutoff, and annotated
555 the clusters with miRBase (v22 all land plant miRNAs (Kozomara et al., 2019);
556 Supplemental Dataset 7). This resulted in 911 clusters; 392 of which are present in two
557 or more species, 172 that are conserved at the genus level (i.e. *Solanum*-conserved,
558 *Petunia*-conserved, and *Nicotiana*-conserved), and only 12 that are conserved across
559 all seven species in this study (Supplemental Dataset 7; Figure 3B-C). The 12
560 conserved clusters can be further condensed into a handful of known miRNA families
561 based on annotations that are broadly conserved across the land plants (e.g. -
562 miR156/157, miR164, miR169/miR399, miR171, miR399, miR165/166/168, and
563 miR172, miR482/miR2118 (Axtell and Meyers, 2018). We designated clusters that
564 could not be annotated with miRBase as “novel.” The majority of these novel clusters
565 appear to be newly-evolved, species-specific miRNAs, while the majority of clusters that
566 are conserved across multiple species (present across ≥ 3 species) aligned with
567 annotated miRNAs in miRBase. In agreement with previous studies showing that
568 lineage-specific miRNAs tend to be weakly expressed relative to conserved miRNAs,
569 we found that the expression of conserved miRNAs was significantly higher on average

570 relative to novel miRNAs (Supplemental Figure 3; benthi p-value = 0.00057903, pepper
571 p-value = 1.98548E-08, potato p-value = 1.97921E-06, tomato p-value = 2.27413E-07,
572 petunia p-value = 2.39254E-05, tobacco p-value = 5.89638E-08; (Axtell et al., 2007)).
573

574 **Solanaceae-specific miRNA family miR5303 is derived from MITE loci**

575 Among the most conserved miRNA groupings, we identified three clusters containing a
576 Solanaceae-specific miRNA, miR5303 (Gu et al., 2014). With the exception of petunia,
577 the miR5303 family was present in relatively high copy numbers across the
578 Solanaceous genomes (7 to 11 miRNAs in each species; Supplemental Dataset 4). It is
579 rare for miRNAs to be present in such high copy numbers; however, our findings are
580 congruent with a previous study that identified a high number of miR5303 copies in
581 tomato, potato, eggplant, and pepper (Gu et al., 2014). To correctly identify miR5303
582 family members, we first aligned all miR5303 variants in miRBase v22 (Figure 4), and
583 found that most of the variants are 24-nt in length, which again, is atypical for a bonafide
584 miRNA family (Meyers et al 2008; Fig 4A). We identified nine miR5303 variants that are
585 21-nt in length in our tomato predictions that have ≥ 75% similarity with miR5303
586 miRBase entries, and found that six of these tomato miRNAs clustered into a family
587 containing a conserved 5' - UUUUG consensus sequence (highlighted by yellow
588 rectangles in Fig 4B). To further characterize the function of this family, we performed a
589 miRNA target prediction analysis using all coding sequences in the tomato genome as
590 putative targets. We found that miR5303 family members are predicted to target
591 thousands of genes in the tomato genome, which again, is unusual for a miRNA family
592 (Supplemental Dataset 8). Given the presence of 24 nucleotide mature miRNA variants
593 that are reminiscent of 24-nt siRNAs, and the perfect/near perfect folding of miR5303
594 precursor sequences that are often formed by inverted repeats (Figure 4C), we decided
595 to test whether miR5303 actually originates from miniature inverted-repeat transposable
596 elements (MITEs) in Solanaceae genomes. Notably, MITEs exist in high copy numbers,
597 can form hairpin sequences that are structurally similar to miRNAs, and are known to
598 generate 24-nt siRNAs (Kuang et al., 2009). To test whether miR5303 family members
599 originated from MITEs, we blasted precursors of miR5303 from tomato against a plant
600 MITE database (Chen et al, 2013) and found that they align perfectly with annotated

601 MITEs, with the miR5303 mature miRNA variants mapping to the terminal inverted
602 repeat (TIR) ends of the MITEs (Figure 4D). We therefore conclude that miR5303 is not
603 a miRNA, but a MITE.
604

605 **Identification of 21-nt *PHAS* loci support genus-level conservation of phasiRNA**
606 **biology**

607 We applied two bioinformatic tools: PHASIS (Kakrana *et al.* 2017) and ShortStack
608 (Axtell 2013), to assemble a list of 21-nt *PHAS* loci across the Solanaceae. To classify
609 coding versus non-coding phasiRNAs we merged PHAS locus coordinates with gene
610 annotation files for each species. Some of the lesser studied Solanaceae genomes
611 have incomplete annotations which resulted in an overprediction of non-coding loci for
612 petunia, pepper, and benthi. To correct this imbalance, we used BLAST to align all non-
613 coding *PHAS* loci to the nr database (Altschul et al., 1990), and manually annotated loci
614 that aligned to protein-coding, rRNA, and non-coding RNA sequences (Figure 5;
615 Supplemental Dataset 4). *PHAS* loci are typically triggered by 22-nt miRNAs that have a
616 5' Uracil bias (Chen et al., 2010; Cuperus et al., 2010). To identify putative triggers for
617 21-nt phasiRNA production, we ran target predictions using our list of mature 22-nt
618 miRNAs plus miR390 as triggers and predicted *PHAS* loci as targets (Supplemental
619 Dataset 9).

620 PhasiRNAs are predominantly generated from transcripts of genes encoding disease
621 resistance-related NB-LRRs, pentatricopeptide repeat (PPR) proteins, MYB
622 transcription factors, and trans-acting siRNA (*TAS*) loci (Liu et al., 2020; Shivaprasad *et*
623 *al.* 2012). We identified 2-3 times more *PHAS* loci in *Solanum* (tomato and potato) and
624 *Capsicum* (pepper) species than *Nicotiana* and *Petunia* (Figure 5). The majority of these
625 *Solanum*/*Capsicum* loci were derived from disease resistance-related genes (Figure
626 5A); this list includes *TAS5*, a recently discovered *NB-LRR* locus that functions in
627 pathogen response in tomato (Canto-Pastor et al.). In contrast, the *Nicotiana* and
628 *Petunia* genomes expressed relatively few disease resistance related phasiRNAs
629 (Figure 5A). We also found a substantial number of non-coding loci that we decided to
630 examine in further detail with the goal of uncovering novel *TAS* loci within the
631 Solanaceae. As a quality control, we confirmed that *TAS3*, a deeply-conserved non-

632 coding phasiRNA, was detected in all of our species datasets (Supplemental Dataset 4;
633 (Xia et al., 2013)). Most notably, we discovered a previously uncharacterized, non-
634 coding locus in both tomato and potato (Figure 5B). This locus is >80% conserved
635 between the two species (Figure 5C) and generates highly abundant 21-nt siRNAs,
636 some of which putatively target genes encoding MYB transcription factors (Figure 5D).
637 We performed a BLAST alignment between the tomato *PHAS* locus and all other non-
638 coding *PHAS* loci to determine whether this locus exists outside of Solanum. This
639 search failed to uncover any significant alignments, indicating that this novel phasiRNA
640 evolved after Solanum split from other genera in the Solanaceae (Särkinen et al., 2013).

641 As mentioned above, PPR-derived *PHAS* loci are abundantly expressed in other
642 species. In our analysis, we only identified two PPR-related *PHAS* loci in the
643 Solanaceae: one in tomato (Solyc10g076450) and one in potato
644 (PGSC0003DMG400020556). We did, however, find strong evidence for another, well-
645 described siRNA mechanism for the transcriptional regulation of PPR genes, in which
646 non-coding TAS-like-1/2 (TASL-1/2) loci are triggered by miR7122, generating 21-nt
647 products that in turn target, and likely silence, PPR genes (Xia et al., 2013). We
648 identified TASL1/2 and its associated miR7122 trigger in both *Nicotiana* species (benthi
649 and tobacco). As demonstrated in other species, major 21-nt products from these TASL
650 loci target PPR genes (Supplemental Figure 4). Surprisingly, we found no evidence for
651 TASL1/2 and its miR7122 trigger in other Solanaceae genera. Given the conservation of
652 this locus in other eudicots outside of the Solanaceae family, we hypothesize that
653 miR7122-TASL1/2 is conserved in *Nicotiana* and was independently lost from the other
654 genera in the nightshade family (Xia et al., 2013).

655 To investigate whether *PHAS* loci are generated from orthologous genes across
656 species, we constructed gene orthogroups and searched for conserved *PHAS* loci
657 within these orthogroupings (Supplemental Dataset 6). Overall, this analysis yielded
658 surprisingly few orthologous *PHAS* loci within the Solanaceae. We did, however,
659 discover that *DICER-LIKE2* (*DCL2*) is a broadly present phasiRNA-producing locus
660 expressed in all of the species in our study (Figure 6). Interestingly, this *PHAS* locus
661 has been previously reported in the Fabaceae, where it is triggered by different miRNAs

662 in medicago and soybean, indicating convergent evolution of phasiRNA production at
663 *DCL2* (Zhai et al., 2011). A *DCL2 PHAS* locus has also been identified in tomato
664 (Canto-Pastor et al. 2019); however, this is the first instance of its widespread presence
665 across the nightshade family. As reported earlier in the results, *DCL2* has expanded
666 through tandem duplications that are shared in the tomato, potato, and pepper genomes
667 (Figure 2). We found the genomic regions containing these tandem *DCL2* paralogs to
668 be structurally conserved on *Solanum* chr11/*Capsicum* chr12 (Figure 6A). Recently, a
669 DCL2-dependent miRNA (miR6026) was validated as a trigger for phasiRNAs derived
670 from the *DCL2* locus in tomato (Wang et al., 2018), creating a negative feedback loop
671 on *DCL2*. To investigate whether the same miRNA triggers initiate *DCL2* phasiRNA
672 production in the rest of the Solanaceae, or, as in the Fabaceae (Zhai et al., 2011),
673 independent triggers evolved at this locus, we looked for shared miRNA-*PHAS* locus
674 interactions. We identified a conserved target site with a strong target score for
675 miR10533 in tomato, potato, pepper, and petunia (Figure 6B). Like miR6026, miR10533
676 is also dependent on DCL2 for its biogenesis (Wang et al., 2018). However, unlike in
677 the Fabaceae, where phasiRNA production proceeds immediately after the miRNA
678 target site (Zhai et al., 2011), *DCL2* phasiRNAs are produced both upstream and
679 downstream of the miR10533/miR6026 target sites in the Solanaceae (Figure 6A). This
680 imprecise initiation of phasing either indicates that there are additional miRNA triggers
681 for this locus, or we are seeing the product of trans-triggering from 22-nt siRNAs that
682 are generated by neighboring *DCL2* paralogs (Figure 6B).

683

684 **hc-siRNAs and transposable elements across SOL genomes**

685 Transposable elements (TEs) are recognized as one of the major evolutionary forces
686 that can shape genomes, via mutations and genome rearrangements. Presumably as
687 protection from the possible detrimental consequences generated by TEs, plants have
688 evolved a mechanism using 24-nt heterochromatic siRNAs (hc-siRNAs) that methylate
689 and repress TEs (Ahmed et al., 2011; Wang et al., 2013). In order to analyze the hc-
690 siRNA landscape in Solanaceae, we first identified TEs in all the available genomes.
691 We observed that TEs represent between 25% (in petunia) and 48% of the genome (in
692 benthi) (Supplemental Figure 5). As expected, the majority of TEs belong to an

693 abundant LTR retrotransposon family, with most LTRs mapping specifically to
694 Gypsy/Ty3 and Copia/Ty1 elements (Galindo-González et al., 2017) (Supplemental
695 Figure 5A). Previous work mapped an expansion of LTRs in the Pepper genome; our
696 results indicate that this observation applies broadly across the Solanaceae, and is
697 likely a generalized signature of Solanaceous genomes (Park et al., 2012; Vicient and
698 Casacuberta, 2017). After identifying TEs we analyzed the number of 24-nt reads that
699 originate from each of the transposon superfamilies. Due to the repetitive nature of TEs,
700 we did not attempt to further classify the sRNA reads into TE subfamilies. We observed
701 that most of the sRNA reads mapped to retrotransposons, including LTR and non-LTR
702 TEs (Supplemental Figure 5B). However, we were surprised to find that a large portion
703 of hc-siRNAs also mapped to SINE elements. SINE elements comprise a unique subset
704 of TEs; they are transcribed by RNA polymerase III, do not encode proteins, and are
705 widespread in almost all multicellular eukaryotic genomes, with the exception
706 Drosophila (Kramerov and Vassetzky, 2011). Our discovery of SINE-derived hc-siRNAs
707 indicates that similar to LTRs, the spread of non-autonomous SINE elements is
708 repressed via hc-siRNA-directed methylation.
709
710 Next, we analyzed the distribution of hc-siRNAs across Solanaceous genomes. We
711 focused this analysis on tomato, pepper, potato and tobacco, which all have
712 chromosome-scale assemblies. As expected, we found relatively high accumulation of
713 hc-siRNAs along the telomeric ends of chromosomes; these hc-siRNAs promote
714 telomere methylation in an RdDM–dependent manner (Vrbsky et al., 2010). We also
715 observed a striking lack of hc-siRNAs across the entire potato genome (Figure 7). This
716 result is similar to a previous observation described in strawberry, where, as in potato,
717 asexual cloning is the primary means of propagation. Clonally propagated strawberry
718 accumulates very low levels of DNA methylation relative to sexually propagated plants
719 (Niederhuth et al., 2016). In the same way, we postulate that depleted hc-siRNA levels
720 in potato could be caused by repeated rounds of asexual propagation. Further studies
721 comparing sexually versus asexually propagated potato varieties would help resolve the
722 connection between mode of reproduction and whether circumventing meiosis over
723 multiple generations leads to degeneration of RdDM-directed methylation.

724

725 **Discovery of 22 nucleotide clusters expressed in response to Geminivirus**
726 **infection**

727 In an exploratory analysis, we found a cluster of 22-nt sRNA reads mapped to a 4.8 kb
728 region in the *S. lycopersicum* genome, and that this cluster is present in a ToLCV-
729 infected sample of *S. lycopersicum* cv. Pusa Ruby and a TYLCV-infected sample of cv.
730 Moneymaker, but absent from the respective mock-treated controls (Figure 8,
731 Moneymaker data not shown). This cluster of 22-nt sRNA expression contains a
732 *DISEASE RESISTANCE PROTEIN* (Solyc05g005330.3.1) and *ABSCISIC ALDEHYDE*
733 *OXIDASE 3* (Solyc05g005333.1.1). To investigate whether there are additional 22-nt
734 clusters that are specifically expressed in response to ToLCV/TYLCV infection, we
735 applied a genome-wide analysis for clusters of 22-nt sRNAs. Using the aforementioned
736 two infected and two control samples, we identified 1,521 22-nt sRNA clusters in total,
737 390 of which passed our filtering criteria (Supplemental Figure 6 and Supplemental
738 Dataset 10). Twenty two of the clusters were induced by more than 4-fold in both
739 cultivars in response to viral infection (Supplemental Figure 6B and Supplemental Table
740 2). Apart from the cluster shown in Figure 6A & B, one prominent example is the two
741 clusters shown in Figure 6C & D, which are induced by ToLCV infection in cv. Pusa
742 Ruby by approximately 1,000-fold and induced by TYLCV infection in cv. Moneymaker
743 by approximately 10,000-fold. These clusters overlap with three gene copies of *EIN3-*
744 *BINDING F-BOX PROTEIN 1* (Solyc05g008700.2.1, Solyc05g008720.1.1, and
745 Solyc05g008730.1.1), one *MYZUS PERSICAE-INDUCED LIPASE 1*
746 (Solyc05g008710.1.1), and one *RNA-DEPENDENT RNA POLYMERASE*
747 (Solyc05g008740.1.1). Further studies are needed to test whether these Geminivirus-
748 induced 22-nt sRNA clusters have a functional role in plant defense, or are potentially
749 induced by the viral pathogen.

750

751

752 **DISCUSSION**

753

754 The Solanaceae family is widely used as a model for studying the evolutionary
755 diversification of specialized metabolism (Fan et al., 2019), morphology (Koenig and
756 Sinha, 2007; Martinez et al., 2020), fruit development (Klee and Giovannoni, 2011), and
757 biotic and abiotic stress tolerance. In this study, we took advantage of the numerous
758 publicly-available sRNA datasets that have been generated for the family to explore
759 unique aspects of sRNA biology within the Solanaceae. We found several features that
760 are shared amongst diverse Solanaceous species including a Solanales-wide
761 duplication of sRNA biogenesis machinery, a previously-annotated Solanaceae-specific
762 miRNA family that we show is actually a MITE-derived miRNA-like siRNA, and DCL2-
763 derived 21-nt phasiRNAs that are broadly expressed across the diverse taxa in our
764 study. We also found several phenomena that evolved within sub-family lineages of the
765 Solanaceae. We discovered a *Nicotiana*-specific expansion of novel miRNAs, a distinct
766 split in the number and types of phasiRNAs that are produced in the *Capsicum/Solanum*
767 versus the *Petunia/Nicotiana* branches of the family, a dramatic depletion of 24-nt hc-
768 siRNAs in asexually propagated potato, and 22-nt siRNA clusters that accumulate in
769 response to viral infection in tomato. Below, we discuss some of the evolutionary
770 implications for Solanaceae-wide and sub-family specific sRNA phenomena that we
771 discovered in this study.

772

773 **Expansion and subfunctionalization of sRNA biogenesis machinery within the**
774 **Solanaceae**

775 In our reconstruction of sRNA biogenesis machinery machinery gene trees, we
776 uncovered lineage-specific expansions of *AGO1*, *AGO2* and *DCL2* gene families. While
777 *AGO1* increased in copy number across the Solanaceae, *AGO2* and *DCL2* specifically
778 expanded in the *Solanum*, and *Solanum/Capsicum* branches of the family, respectively,
779 through tandem duplications. The tandem *DCL2* paralogs have been previously
780 characterized to function as part of the tomato viral defense response (Wang et al.,
781 2018), discussed in further detail below. Using public expression data for tomato, we
782 identified distinct expression patterns in vegetative and reproductive organs for *DCL2*

783 paralogs, with enriched abundance in reproductive organs, suggesting that these gene
784 paralogs are undergoing subfunctionalization. Recent studies show that 24-nt
785 phasiRNAs are produced only in reproductive organs of angiosperms, while 21-nt
786 phasiRNAs are produced in both vegetative and reproductive tissues (Xia et al, 2019,
787 Pokhrel et al., 2020). The 24-nt reproductive phasiRNAs are triggered by miR2275 in
788 most of the angiosperms while in Solanaceous species, the miRNA trigger remains
789 unknown (Xia et al, 2019, Pokhrel et al, 2021). Given that *DCL2* was shown to process
790 endogenous 22-nt miRNAs, and that the expression of some *DCL2* paralogs peak in
791 reproductive organs, it would be interesting to functionally test whether this *DCL2*
792 paralog expressed in reproductive tissues specifically processes a 22-nt miRNA that
793 triggers reproductive 24-nt phasiRNA biogenesis.
794
795 **Solanaceae-wide miR5303 cluster is derived from MITEs**
796 Our cross-species miRNA predictions and clustering revealed 12 family-wide clusters of
797 miRNAs. While the majority of these clusters are associated with deeply-conserved land
798 plant miRNA families that are shared outside of the Solanaceae, we investigated the
799 Solanaceae-specific cluster annotated as miR5303 (Mohorianu et al., 2011). We
800 discovered that this family exhibits many features that are atypical of miRNAs. For
801 example, related miR5303 sequences in miRBase include both 21-nt and 24-nt mature
802 sequences and most of the Solanaceae genomes harbor relatively high copy numbers
803 of miR5303 isomiRs that putatively target thousands of genes based on our miRNA-
804 target prediction analysis. We found that, similar to a previous study on MITE-derived
805 miRNA-like siRNAs, mature miR5303 “miRNA” sequences align perfectly to the terminal
806 inverted repeat (TIR) region of Solanaceae MITEs. (Kuang et al., 2009). How did our
807 miRNA prediction pipeline lead to the identification of MITE-derived sRNAs? MITEs
808 have near perfect hairpin folding and express sRNAs within mature miRNA size ranges,
809 and thus fit many of the criteria used to predict novel miRNA precursors. It has been
810 proposed that MITEs may contribute to the *de novo* evolution of miRNAs. However, this
811 model is somewhat controversial, as MITEs tend to express imprecise sRNAs that are
812 variable in both length and sequence, and thus are more likely the products of siRNA
813 rather than miRNA biogenesis machinery (Cui et al, 2017). Even so, the conspicuous

presence of miR5303-related sRNAs exclusively in the Solanaceae is intriguing, and further investigation into putative functional roles for these siRNAs could be interesting.

DCL2 is a broadly expressed _PHAS_ locus that may control viral responses across the Solanaceae

In a previous study focused on mechanisms of viral resistance in tomato, paralogous copies of *DCL2* were shown to process a 22-nt miRNA (miR6026) that has dual functions, participating in antiviral responses and creating a self-regulating feedback loop by triggering *DCL2* phasiRNA production (Wang et al., 2018). In this study we identified *DCL2* as a widely-expressed *PHAS* locus that is present in all seven Solanaceous species in our study. Contrary to previous characterization of this locus, we predicted that another 22-nt miRNA, miR10533, triggers phasiRNA production in *Solanum*, *Capsicum*, and *Petunia* genera. Similar to miR6026, miR10533 targets disease resistance-related genes in addition to *DCL2* (*PHAS* target predictions table). Based on the accumulation patterns of *DCL2* phasiRNAs, neither miRNA appears to be an obvious trigger, although target mimic experiments with miR6026 showed reduced *DCL2* phasiRNA production (Wang et al., 2018). We identified the miR6026 site more than 250 bp outside of our predicted phasiRNA production region, whereas miR10533 is sandwiched within the phasiRNA register (Figure 6). The lack of an obvious trigger suggests two possibilities: 1) there may be another, as yet unidentified miRNA trigger, and/or 2) as hypothesized by previous authors, the 22-nt sRNA products generated from the *DCL2* paralogs may be cross triggering one another in *cis*, creating multiple phasiRNA initiation sites (Wang et al., 2018). We have likely saturated miRNA predictions for tomato, given the depth of sRNA sequence data available for this species, and thus it is unlikely that we are simply missing an additional trigger for *DCL2* phasiRNA production. Consistent with the second hypothesis, we observed weaker phasing scores across most of the *DCL2 PHAS* loci, indicating that cross-locus regulatory interactions trigger phasiRNA production across *DCL2* loci.

DCL2 PHAS loci have also been identified in two different Fabaceae models, soybean and medicago, where they are triggered by independent miRNAs (Li et al., 2010; Zhai et

845 al., 2011). Our study, in combination with this previous work, shows that phasiRNA
846 target-trigger interactions around *DCL2* have evolved multiple times within and across
847 eudicot families. This evolutionary hotspot for phasiRNA production fits into a model in
848 which the expression of sRNA biogenesis machinery is regulated via self-triggered
849 phasiRNA production. Depending on the species, different components of sRNA
850 biogenesis machinery are processed into *PHAS* loci. In soybean, for example, *SGS3* is
851 targeted for phasiRNA production (Song et al., 2011), and in Arabidopsis, *AGO1* and
852 *DCL1* are both processed into *PHAS* loci (Xie et al., 2003; Vaucheret et al., 2004). Why
853 do plants use post-transcriptional regulation to control siRNA biogenesis machinery?
854 One potential theory is that by regulating sRNA biogenesis machinery at the post-
855 transcriptional level, plants can maintain a standing pool of transcripts for sRNA
856 biogenesis that can be rapidly released and translated in response to pathogens.
857
858 **Lineage-specific expression of miRNAs and phasiRNAs**
859 One of our goals in this study was to identify miRNAs that are uniquely conserved within
860 the Solanaceae; however, as discussed above, we demonstrate that miR5303, the only
861 Solanaceae-specific "miRNA family" that we were able to predict in all of our study
862 species, is actually a MITE-derived siRNA. Rather than uncovering broadly conserved
863 miRNAs, we discovered numerous instances of lineage-specific miRNAs, with the most
864 pronounced example coming from our representative species for *Nicotiana*. Even after
865 stringent filtering, we predicted over 350 miRNAs in the benthi genome, with more than
866 half of these comprising previously unannotated, lineage-specific miRNAs. Congruent
867 with previous observations, we show that these lineage-specific miRNAs are generally
868 expressed at lower levels than deeply conserved family members (Supplemental Figure
869 3) (Axtell et al., 2007). There are, however, a handful of newly annotated miRNAs that
870 are abundantly expressed (>1,000 rpm; Supplemental Figure 3). Given the ease of
871 agrobacterium infiltration in benthi, followup studies using transiently expressed target
872 mimic knockdowns and PARE sequencing may provide new insight into the targets and
873 putative functions of these rapidly-evolving *Nicotiana*-specific miRNAs. One bottleneck
874 that we encountered in this analysis was a lack of deep sRNA sequence data for
875 tobacco. Despite the lack of sampling in tobacco, we still predicted more than 150

876 miRNAs for this genome, which is similar to the number of miRNAs that we found in the
877 tomato genome, despite having almost 10 times more sRNA sequence data for tomato.
878 We are likely looking at the tip of the iceberg when it comes to miRNA discoveries in
879 tobacco, and we predict that deeper sequencing in tobacco and related *Nicotiana*
880 species will facilitate big gains when it comes to miRNA discovery in the Solanaceae.
881
882 In a reverse trend, our genome-wide 21-nt phasiRNA predictions uncovered relatively
883 few *PHAS* loci for *Nicotiana* and *Petunia* species compared to the *Solanum/Capsicum*
884 branch of the family (Figure 5A). A distinct lack of *PHAS* loci encoding NB-LRRs in
885 *Nicotiana* and *Petunia* accounts for one of the biggest differences in the number of
886 *PHAS* loci between these two branches of the family. We also discovered two strongly
887 expressed non-coding *PHAS* loci that are conserved at the sub-family level. One is
888 conserved in both benthi and tobacco, and was previously described to function in the
889 post-transcriptional regulation of PPR genes (Supplemental Figure 4) (Xia et al., 2013).
890 The other locus is uncharacterized, and specific to tomato and potato (Figure 5B). We
891 discovered that this new *PHAS* locus produces a prominent 21-nt siRNA that putatively
892 targets MYB transcription factors (Figure 5D). It would be interesting to test whether this
893 Solanum-specific *PHAS* locus really does function in regulating the expression of MYB
894 transcription factors. PhasiRNA production is triggered by miRNAs. Therefore, it is
895 logical that in addition to discovering lineage-specific miRNAs, we also found lineage-
896 specific *PHAS* loci across the Solanaceae.
897
898 **Repressed hc-siRNA expression reflects a history of asexual propagation in**
899 **potato**
900 Our genome-wide hc-siRNA analysis revealed a low abundance of 24-nt TE-associated
901 siRNAs in potato. We hypothesize that this relative depletion in potato is caused by the
902 asexual means of propagation that is common for this crop. Epigenetic marks are
903 faithfully copied during mitosis; however, during meiosis, they are reset by RdDM-based
904 repatterning, which involves TE-derived hc-siRNAs directing DNA methylation (Daxinger
905 et al., 2009; Schoft et al., 2009; Mosher and Melnyk, 2010; Slotkin et al., 2009;
906 Verhoeven and Preite, 2014). Asexual propagation circumvents meiosis, and thus this

907 RdDM-based reseting of epigenetic marks is avoided (Verhoeven and Preite, 2014),
908 and over many rounds of asexual propagation DNA methyl-cytosine marks and their
909 associated hc-siRNAs may become depleted. In line with this hypothesis, a related
910 study investigating genome-wide DNA methylation patterns in diverse species found a
911 stark depletion in CHH cytosine methylation in strawberry, another asexually
912 propagated species (Niederhuth et al., 2016). However, there are limitations to our
913 conclusions regarding depleted hc-siRNAs in potato. These limitations include imperfect
914 sampling, notably, the majority of our potato samples are from vegetative tissues
915 (although this is true for most of the species in this study; Supplemental Dataset 1), and
916 insufficient information about the source tissue that was used to generate these public
917 datasets, particularly information regarding how many generations of asexual
918 reproduction the source tissue underwent prior to sampling. Since sRNA-derived TE
919 silencing gradually accumulates over multiple generations, a well-devised study
920 comparing long-term asexually versus sexually propagated source tissue would help
921 resolve whether levels of RdDM are directly impacted by assexual propagation, and
922 whether these hc-siRNAs could be reactivated during reproductive development.
923
924 **22-nt clusters expressed in response to viral infection in tomato**
925 Recent work in Arabidopsis uncovered 22-nt siRNAs that are expressed in response to
926 environmental stress, and are capable of impacting global translational repression,
927 including the translation of their cognate genes. Moreover, this translational repression
928 is correlated with an inhibition of growth and activation of stress-response pathways
929 (Wu et al. 2020). In this study, we identified similar 22-nt siRNA clusters in tomato that
930 are expressed in response to viral infection. Whether these siRNAs are also involved in
931 attenuating global translation and growth so that more resources can be allocated to
932 antiviral response remains to be seen. Several of the clusters that we identified are
933 generated from genes involved in ABA production and ethylene signaling, indicating that
934 these 22-nt siRNA clusters may coordinate genomic responses to pathogen attack by
935 fine tuning the expression of ABA and ethylene pathways. Future work investigating
936 whether this response is initiated by the plant in order to activate defense mechanisms

937 or perhaps is hijacked by the virus in order to silence antiviral responses would provide
938 insight into the evolutionary function of these distinctive siRNAs.
939
940 **CONCLUSION**
941 In conclusion, while genera within the Solanaceae share unifying features in the
942 evolutionary history of their sRNA biology, there are many lineage-specific phenomena
943 that are not broadly shared across the family. This conclusion is important as it provides
944 valuable information on the appropriateness of a given model species for providing
945 generalized insights into sRNA biology. Simultaneously, we encountered limitations due
946 to disparate sampling within the Solanaceae. For example, while sample data exist
947 across developmental stages, environments, and genotypes to support investigations
948 into tomato sRNA biology, there is a lack of publicly-available resources to study
949 tomato's sister species, eggplant (Chapman, 2019). Similarly, our understanding of
950 sRNA biology for *Petunia hybrida* is largely limited to reproductive samples. Given the
951 sub-family phenomena that we identified in this study, we suggest that delving into
952 under-sampled taxa rather than increasing sampling in well-studied species will yield a
953 greater return on investment when it comes to discovering new aspects of sRNA biology
954 within the Solanaceae.
955
956 **LARGE DATASETS**
957 Supplemental Dataset 1 – SRA Sample Processing
958 Supplemental Dataset 2 – Solanaceae TEs
959 Supplemental Dataset 3 – miRNAs Annotated by Species
960 Supplemental Dataset 4 – phasiRNAs Annotated by Species
961 Supplemental Dataset 5 – Solanaceae Orthogroups
962 Supplemental Dataset 6 – Benthi structVis Filtering
963 Supplemental Dataset 7 – Solanaceae miRNA Families
964 Supplemental Dataset 8 – Tomato miRNA Target Predictions
965 Supplemental Dataset 9 – PHAS Locus miRNA Interactions
966 Supplemental Dataset 10 – Table of 22-nt sRNA Clusters
967

ACKNOWLEDGEMENTS

We thank Rui Xia for generating the annotation file that we used for the pepper (*Capscium annuum*) genome, and Feray Demirci and Deepti Ramachandruni for assistance with aspects of data processing. The work was supported with funding from NSF IOS awards 1842698, 754097 and 1650843, and USDA NIFA award 2019-67013-29010 to Meyers; NSF award 1523668 to M. Frank.

TABLES

Table 1: Reference genomes and software used for bioinformatic analyses

Species	Genome Version	File Source	Analyses
Arabidopsis thaliana	Araport11	Phytozome v13	MUSCLE, IQ-TREE, OrthoFinder
Ipomoea triloba	NSP323_V3 (Wu et al., 2018)	Sweetpotato Genomics Resource	MUSCLE, IQ-TREE, OrthoFinder
Ipomoea trifida	NSP306_V3 (Wu et al., 2018)	Sweetpotato Genomics Resource	MUSCLE, IQ-TREE, OrthoFinder
Capsicum annum	Zunla-1 v2.0 (Qin et al., 2014)	http://public.genomics.org.cn/BGI/pepper/	Expression DB, OrthoFinder, miR-Prefer, ShortStack, PHASIS, MUSCLE, IQ-TREE
Petunia axillaris	V1.6.2 (Bombarely et al., 2016)	ftp://ftp.solgenomics.net/genomes/	Expression DB, miR-Prefer, ShortStack, PHASIS, MUSCLE, IQ-TREE
Petunia inflata	V1.0.1 (Bombarely et al., 2016)	ftp://ftp.solgenomics.net/genomes/	Expression DB, miR-Prefer, ShortStack, PHASIS, MUSCLE, IQ-TREE

Nicotiana tabacum	V4.5 (Edward et al. 2017)	ftp://ftp.solgenomics.net/genomes/	Expression DB, miR-Prefer, ShortStack, PHASIS, MUSCLE, IQ-TREE
Nicotiana benthamiana	V0.3 (Bombarely et al., 2012)	ftp://ftp.solgenomics.net/genomes/	Expression DB, miR-Prefer, ShortStack, PHASIS
Nicotiana benthamiana	V0.4.4 (Bombarely et al., 2012)	ftp://ftp.solgenomics.net/genomes/	MUSCLE, IQ-TREE
Solanum tuberosum	ITAG v1.0 (Potato Genome Sequencing Consortium et al., 2011)	ftp://ftp.solgenomics.net/genomes/	Expression DB, miR-Prefer, ShortStack (miRNA prediction)
Solanum tuberosum	v3.4	ftp://ftp.solgenomics.net/genomes/	MUSCLE, IQ-TREE, Orthogroups
Solanum tuberosum	V4.04 (Hardigan et al., 2016)	http://solanaceae.plantbiology.msu.edu/pgsc_download.shtml	PHASIS, ShortStack (PHAS locus prediction)
Solanum lycopersicum	V3.2	ftp://ftp.solgenomics.net/genomes/	Expression DB, miR-Prefer, ShortStack, PHASIS,
Solanum *lycopersicum*	V2.4 (Tomato Genome Consortium, 2012)	ftp://ftp.solgenomics.net/genomes/	MUSCLE, IQ-TREE
Mimulus guttatus	JGI v2.0 (Hellsten et al., 2013)	https://phytozome.jgi.doe.gov/pz/portal.html#!bulk?org=Org_Mguttatus	miR-Prefer, ShortStack, PHASIS,

Table 2: Summary of annotated *AGO*, *DCL*, *DRB*, *NRP* and *RDR* family members in Solanaceous and outgroup genomes.

Specie	Ploidy*	*AGO*	*DCL*	*DRB*	*NRP*	*RDR*
Arabidopsis thaliana	2n = 2x = 10	10	4	7	3	6
Capsicum annuum	2n = 2x = 24	11	5	4	5	5
Ipomoea triloba	2n = 2x = 30	13	4	7	5	6
Ipomoea trifida	2n = 2x = 30	13	4	7	4	5
Nicotiana benthamiana	2n = 4x = 38	18	4	7	6	7
Nicotiana tabacum	2n = 4x = 48	21	8	7	6	10
Petunia axillaris	2n = 2x = 14	12	4	3	3	4
Petunia inflata	2n = 2x = 14	13	4	5	3	5
Solanum lycopersicum	2n = 2x = 24	13	7	3	2	6
Solanum tuberosum	2n = 2x = 24	15	5	5	1	8

*The ploidy was assessed using the Kew Royal Botanical Gardens database (https://cvalues.science.kew.org)

FIGURE LEGENDS

Figure 1: Solanaceae-specific diversification of the *AGO* family highlights expansion and subfunctionalization of subfamily members. Phylogenetic tree of proteins encoded by the *AGO* gene family in the Solanaceae (A). Clades of *AGO* subfamily members are drawn with distinct colors. Yellow boxes highlight groups of *AGO* genes that have expanded in Solanaceae. Red circles indicate *AGO* homologs in tomatoes. Heatmaps show the relative expression of *AGO1* and *AGO2* from public data (B). Orthologous protein groups were identified using OrthoFinder and SonicParanoid. Protein alignments and phylogeny analysis were completed using MUSCLE and IQ- TREE. Phylogenetic tree was illustrated using iTOL.

Figure 2: Phylogenetic analysis of DCL family members encoded in the Solanaceae highlights a *Solanum*/*Capsicum*-specific expansion of DCL2. Phylogenetic tree of protein sequences indicating *DCL* subfamily members in the Solanaceae (A). Subclades of the *DCL* family are drawn with distinct colors and yellow boxes highlight groups of *DCL2* that expanded

in *Capsicum* and *Solanum* genera. Red circles indicate tomato paralogs for *DCL2*. Heatmaps show the relative abundance of these tomato *DCL2* paralogs in diverse samples (B). Protein orthologous groups were identified using OrthoFinder and SonicParanoid. Protein alignments and phylogeny analysis were done using MUSCLE and IQ- TREE. Phylogenetic tree was visualized using iTOL.

Figure 3: MicroRNA predictions across Solanaceae support a lineage-specific expansion of miRNAs. Venn diagrams of total miRNAs predicted by miRPrefer (red), Shortstack (yellow), and both programs (orange) for each species (A). Upset plots showing novel (B) and known (C) miRNAs that are shared across Solanaceae species. For each Upset plot: the bottom left panel shows the entire size of each set as a horizontal histogram, the bottom right panel shows the intersection matrix, and the upper right panel shows the size of each combination as a vertical histogram. The red line marks miRNAs common to all species, the purple line marks miRNAs common to both *Petunia* species, the orange line marks miRNAs common to both *Solanum* species, the green line marks miRNAs common to both *Nicotiana* species, and the blue and yellow lines mark benthi- and pepper-specific miRNAs, respectively.

Figure 4: miR5303 aligns to MITE terminal inverted repeat (TIR) sequences. The previously-annotated Solanaceae-specific miRNA family, miR5303, exhibits many features that disqualify it as a bonafide miRNA. The majority of the miR5303 miRBase entries include mature sequences that are 24-nt in length, indicating that these sRNAs are likely derived from siRNA producing loci (A). miR5303 miRBase entries are highly variable in their sequence; we identified a consensus sequence to isolate true miR5303 family members (highlighted in the yellow box) (A). We filtered out miRNAs > 22-nt in length; however, our predicted miR5303 family members that are 21 or 22 nt follow the same 5' consensus sequence (UUUUG) as the miRBase entries (B). The predicted precursors of miR5303 family members have near perfect hairpin folding, indicating that these loci are likely inverted repeats, rather than real miRNA precursors (C), and BLAST alignment of miR5303 family members to the plant MITE database shows perfect/near perfect alignment of the precursors to MITE entries, with the mature miRNA sequences aligning to the TIR sequences (D).

Figure 5: Genus-specific trends of 21-nt *PHAS* loci within the Solanaceae. *Solanum* (tomato and potato) and *Capsicum* (pepper) genera produce 2-3 times more PHAS loci and

predominantly express disease resistance-related coding loci, relative to *Nicotiana* (tobacco and benthi) and *Petunia* genera (A). The raw number of loci for each category in (A) is shown in white. All of the species express non-coding PHAS loci (orange). Two previously unidentified non-coding TAS-like loci identified on chromosome 5 in tomato (left) and potato (right) show strong phasing (B) and 83% cross-species sequence conservation (C). An abundant 21-nt product from this novel non-coding *PHAS* locus has sequence complementarity to MYB TFs (D).

Figure 6: *DCL2* phasiRNA-producing loci are conserved across Solanaceous species. *DCL2* paralogs in pepper, tomato, and potato, and orthologs in petunia, benthi, and tobacco all produce 21-nt phasiRNAs (A). We identified conserved miRNA target sites for miR10533 and miR6026 in pepper, tomato, potato, and petunia (red and yellow arrow respectively denotes cleavage sites) that has a strong target score, and may be a conserved mechanism for triggering DCL2 *PHAS* locus production in these species (B).

Figure 7: hc-siRNA expression across chromosomes in Solanaceae. Normalized read counts for 24-nt TE-associated hc-siRNAs are plotted across the assembled chromosomes for tobacco, tomato, potato, and pepper. The x-axis represents the chromosome number, alternating between grey and black, and the y-axis represents the average number of reads at each chromosome position. The average read number was calculated based on the number of available libraries for each species. As expected, the majority of hc-siRNAs map to telomeric ends. Unexpectedly, potato accumulates a low proportion of 24-nt hc-siRNAs relative to total sRNAs.

Figure 8: Tomato genome produces 22-nt sRNA clusters in response to geminivirus infection.
sRNA reads mapped to two genomic regions in an infected-control sample pair are shown. The central red and blue boxes represent gene models from the 3.0 version of *S. lycopersicum* genome, and shaded boxes represent repetitive sequences. Dots represent sRNA reads, color-coded by length, mapped to the genomic region, with abundance represented by the position along the Y axis. Hollow dots are multi-mappers, and solid dots are unique-mappers. (A) and (C) are from a control, mock-infected sample (Sly_leaves_t1) and (B) and (D) are from the

1067 corresponding virus-infected sample (Sly_leaves_t2). (A) and (B) show the genomic region
1068 Ch05:268043..272842. (C) and (D) show the genomic region Ch05:2979082..2987879.
1069
1070
1071

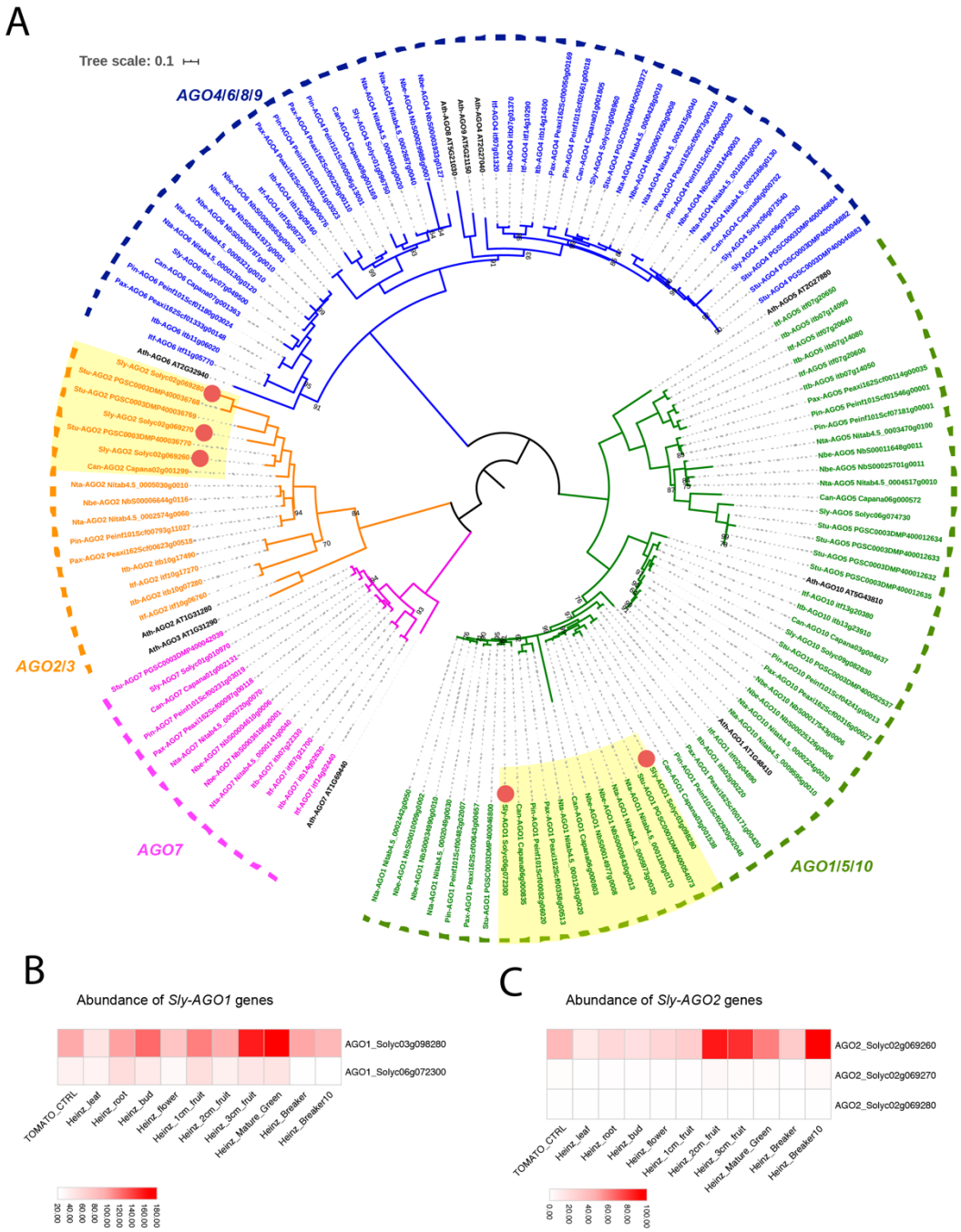

Figure 1: Solanaceae-specific diversification of the *AGO* family highlights expansion and subfunctionalization of subfamily members. Phylogenetic tree of proteins encoded by the *AGO* gene family in the Solanaceae (A). Clades of *AGO* subfamily members are drawn with distinct colors. Yellow boxes highlight groups of *AGO* genes that have expanded in Solanaceae. Red circles indicate *AGO* homologs in tomatoes. Heatmaps show the relative expression of *AGO1* and *AGO2* from public data (B). Orthologous protein groups were identified using OrthoFinder and SonicParanoid. Protein alignments and phylogeny analysis were completed using MUSCLE and IQ-TREE. Phylogenetic tree was illustrated using iTOL.

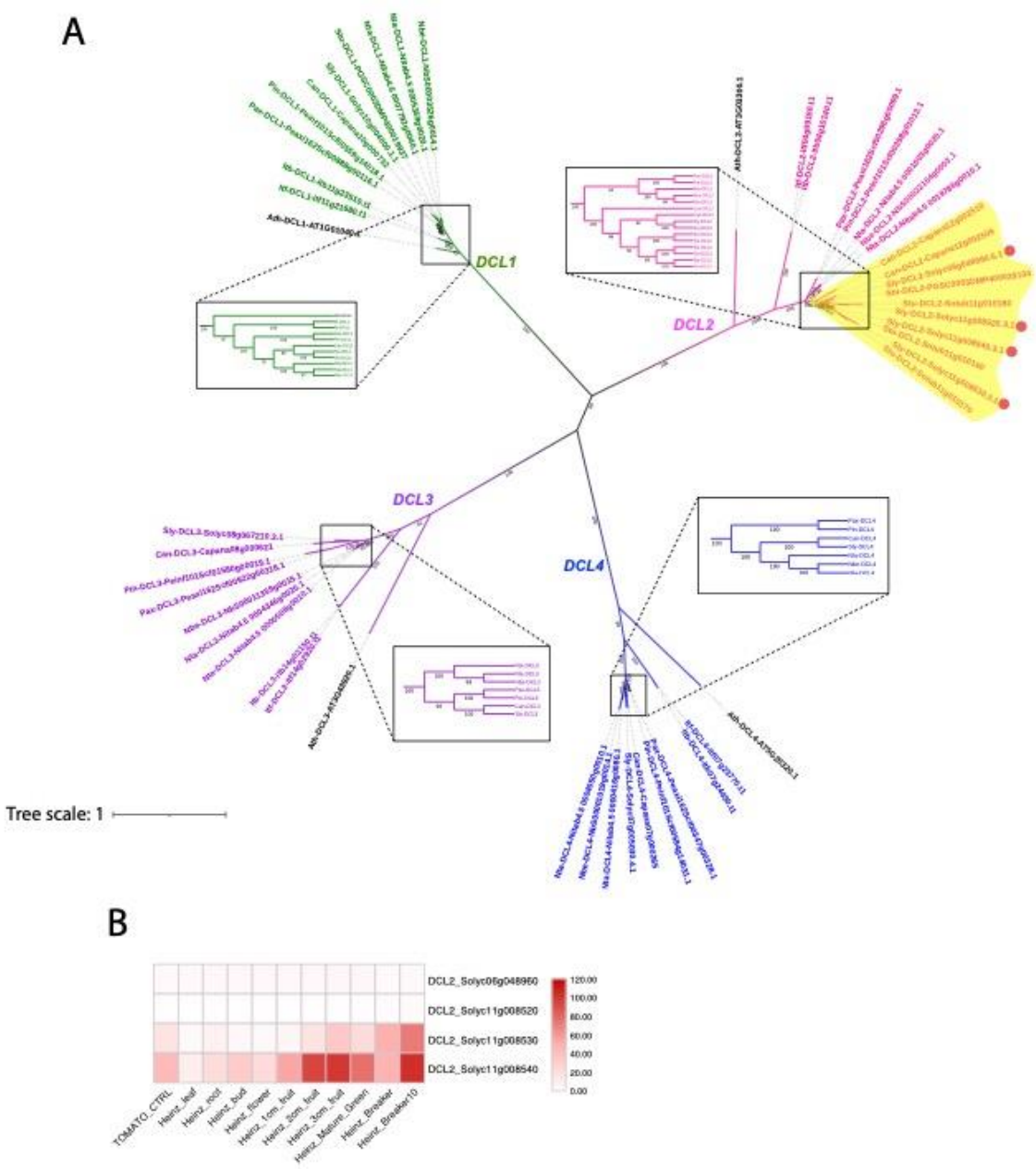

Figure 2: Phylogenetic analysis of DCL family members encoded in the Solanaceae highlights a *Solanum*/*Capsicum*-specific expansion of DCL2. Phylogenetic tree of protein sequences indicating *DCL* subfamily members in the Solanaceae (A). Subclades of the *DCL* family are drawn with distinct colors and yellow boxes highlight groups of *DCL2* that expanded in *Capsicum* and *Solanum* genera. Red circles indicate tomato paralogs for *DCL2*. Heatmaps show the relative abundance of these tomato *DCL2* paralogs in diverse samples (B). Protein orthologous groups were identified using OrthoFinder and SonicParanoid. Protein alignments and phylogeny analysis were done using MUSCLE and IQ- TREE. Phylogenetic tree was visualized using iTOL.

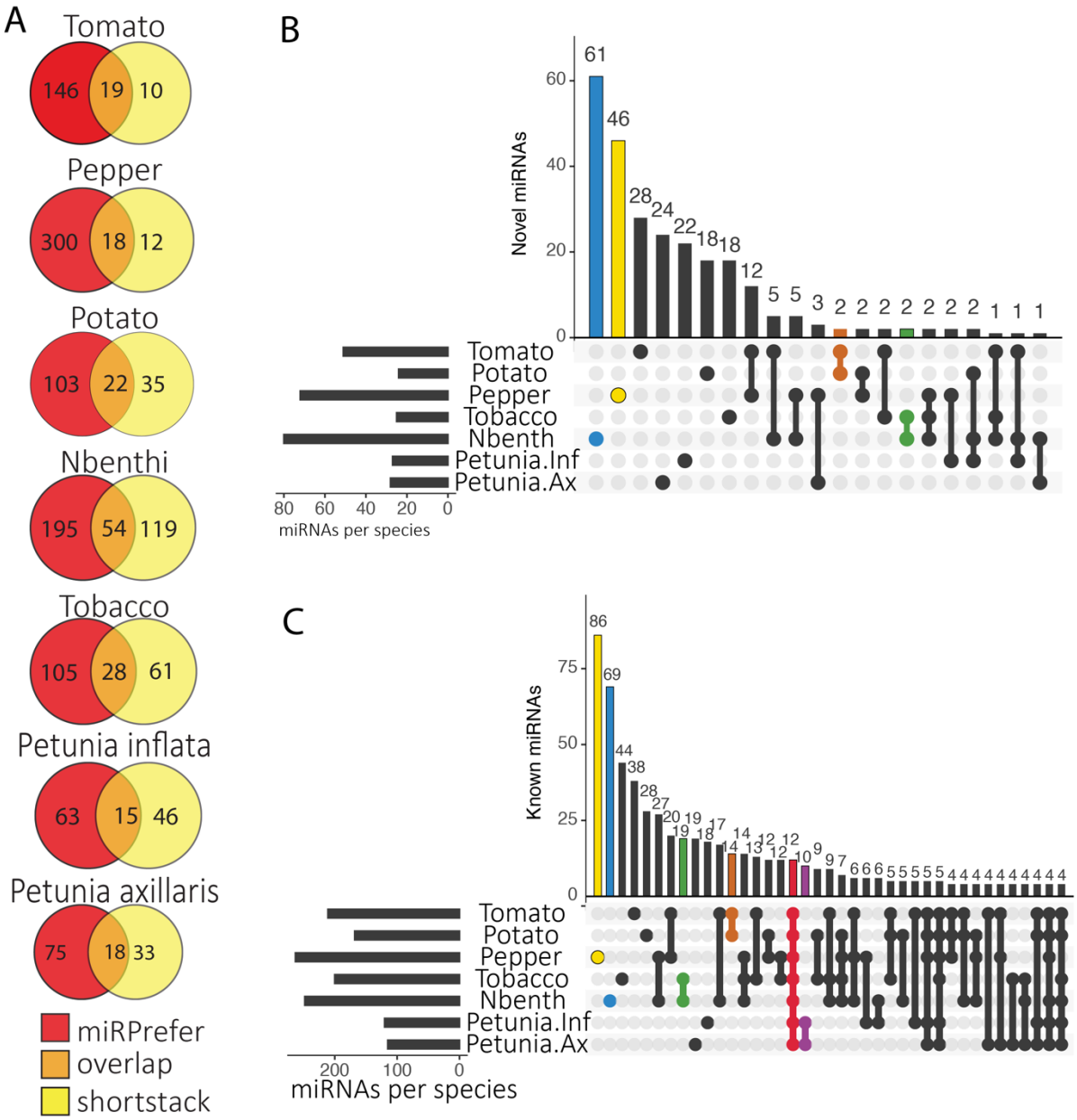

Figure 3: MicroRNA predictions across Solanaceae support a lineage-specific expansion of miRNAs. Venn diagrams of total miRNAs predicted by miRPrefer (red), Shortstack (yellow), and both programs (orange) for each species (A). Upset plots showing novel (B) and known (C) miRNAs that are shared across Solanaceae species. For each Upset plot: the bottom left panel shows the entire size of each set as a horizontal histogram, the bottom right panel shows the intersection matrix, and the upper right panel shows the size of each combination as a vertical histogram. The red line marks miRNAs common to all species, the purple line marks miRNAs common to both *Petunia* species, the orange line marks miRNAs common to both *Solanum* species, the green line marks miRNAs common to both *Nicotiana* species, and the blue and yellow lines mark benthi- and pepper-specific miRNAs, respectively.

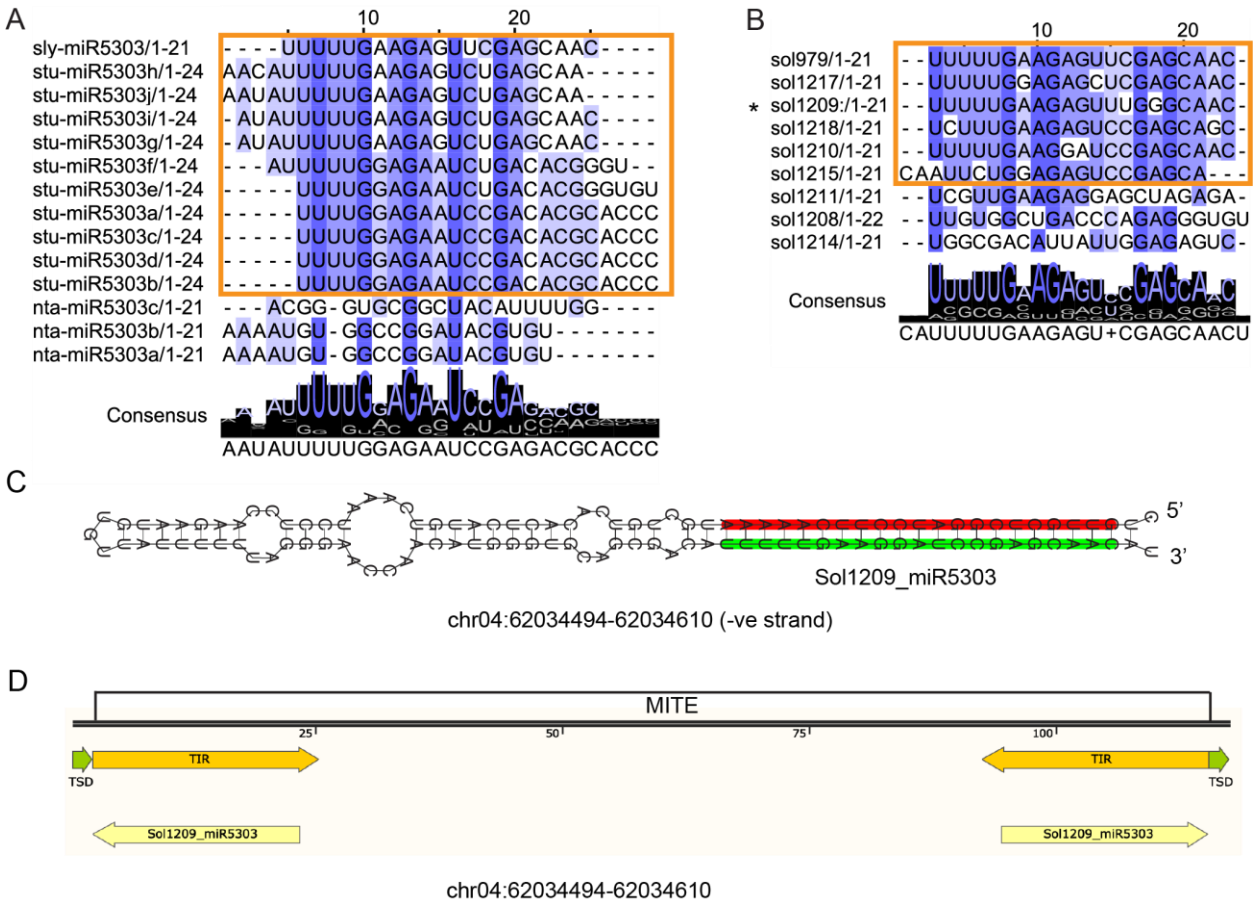

Figure 4: miR5303 aligns to MITE terminal inverted repeat (TIR) sequences. The previously-annotated Solanaceae-specific miRNA family, miR5303, exhibits many features that disqualify it as a bonafide miRNA. The majority of the miR5303 miRBase entries include mature sequences that are 24-nt in length, indicating that these sRNAs are likely derived from siRNA producing loci (A). miR5303 miRBase entries are highly variable in their sequence; we identified a consensus sequence to isolate true miR5303 family members (highlighted in the yellow box) (A). We filtered out miRNAs > 22-nt in length; however, our predicted miR5303 family members that are 21 or 22 nt follow the same 5' consensus sequence (UUUUG) as the miRBase entries (B). The predicted precursors of miR5303 family members have near perfect hairpin folding, indicating that these loci are likely inverted repeats, rather than real miRNA precursors (C), and BLAST alignment of miR5303 family members to the plant MITE database shows perfect/near perfect alignment of the precursors to MITE entries, with the mature miRNA sequences aligning to the TIR sequences (D).

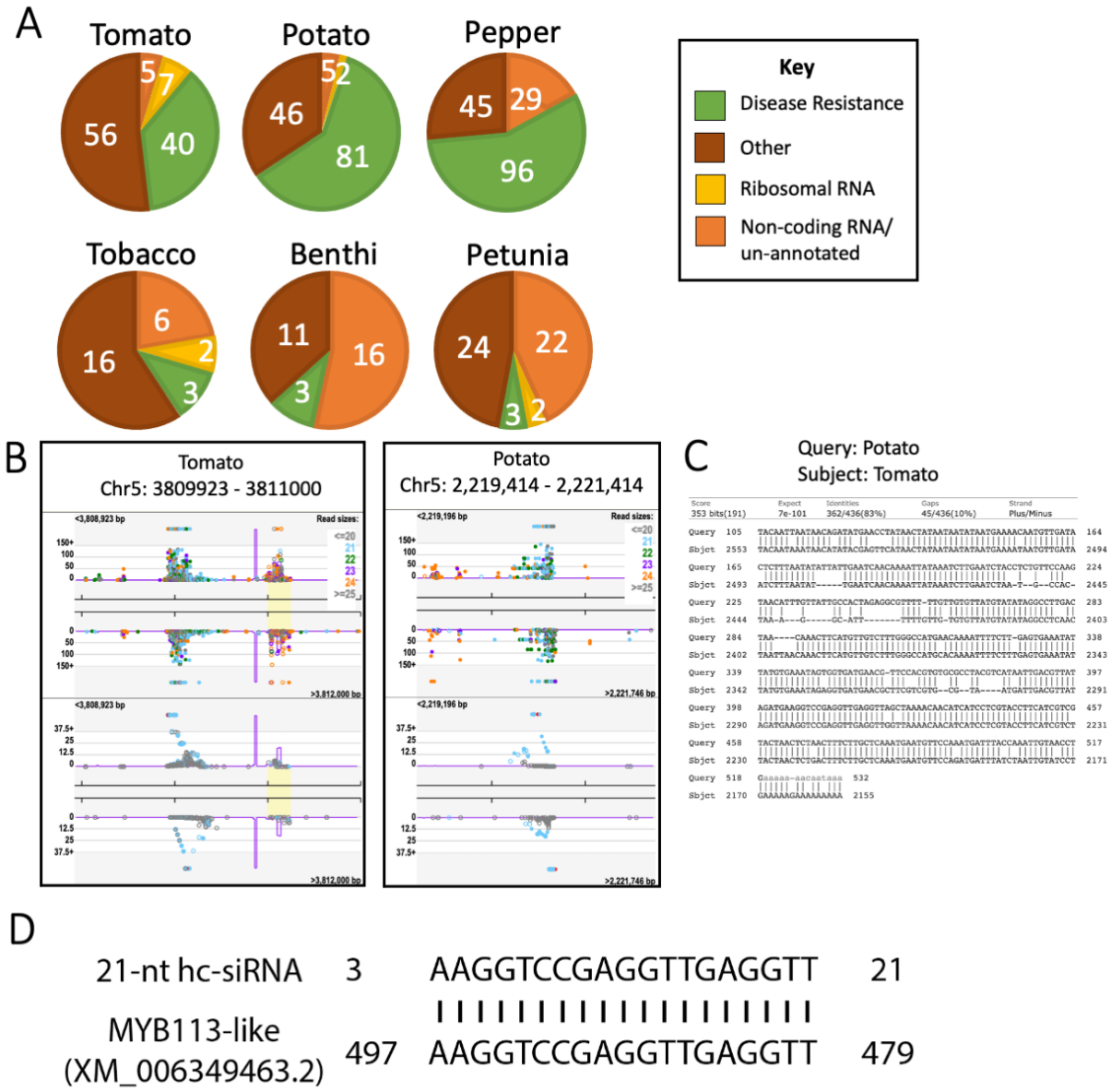

Figure 5: Genus-specific trends of 21-nt *PHAS* loci within the Solanaceae. *Solanum* (tomato and potato) and *Capsicum* (pepper) genera produce 2-3 times more PHAS loci and predominantly express disease resistance-related coding loci, relative to *Nicotiana* (tobacco and benthi) and *Petunia* genera (A). The raw number of loci for each category in (A) is shown in white. All of the species express non-coding PHAS loci (orange). Two previously unidentified non-coding TAS-like loci identified on chromosome 5 in tomato (left) and potato (right) show strong phasing (B) and 83% cross-species sequence conservation (C). An abundant 21-nt product from this novel non-coding *PHAS* locus has sequence complementarity to MYB TFs (D).

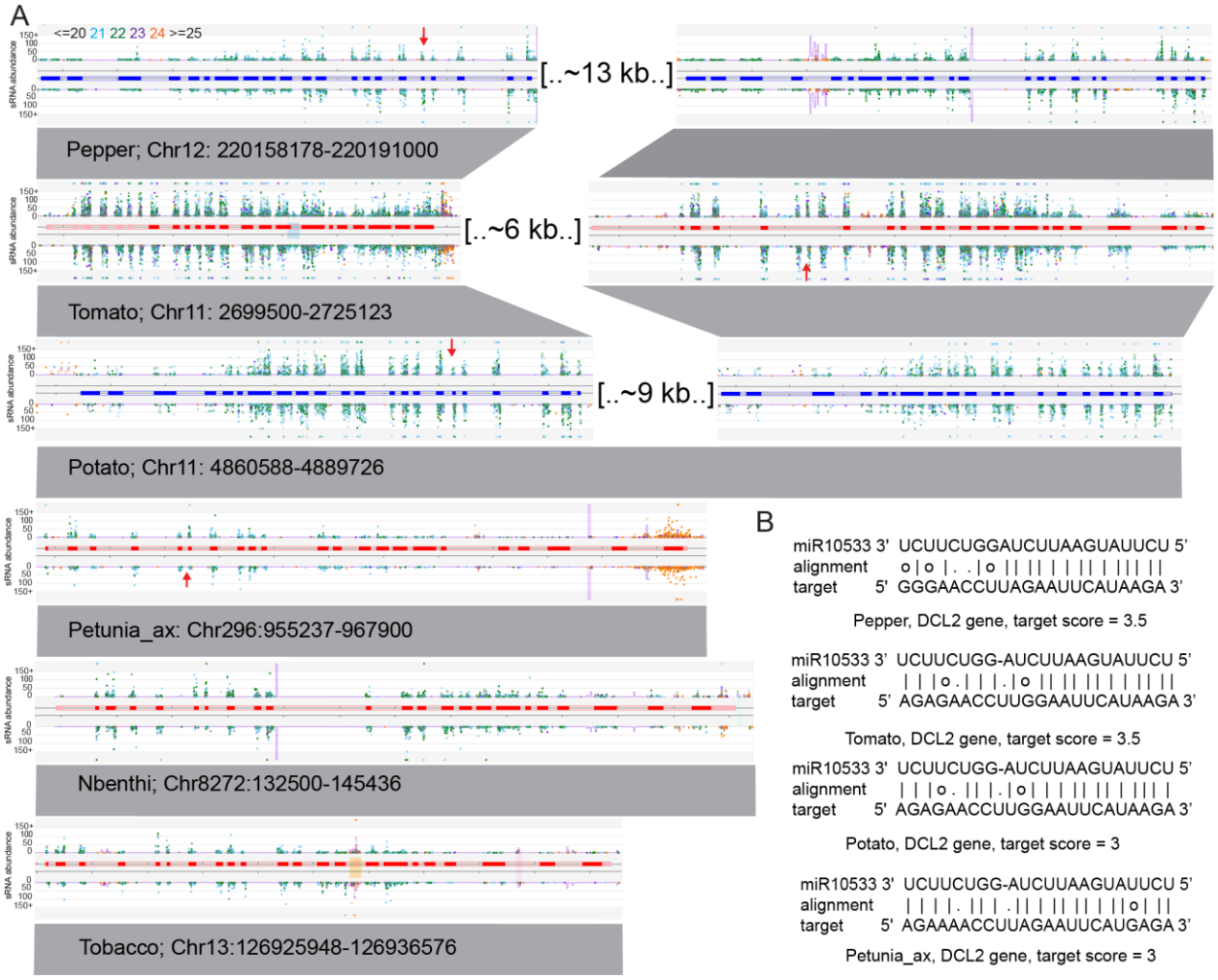

Figure 6: *DCL2* phasiRNA-producing loci are conserved across Solanaceous species. *DCL2* paralogs in pepper, tomato, and potato, and orthologs in petunia, benthi, and tobacco all produce 21-nt phasiRNAs (A). We identified conserved miRNA target sites for miR10533 and miR6026 in pepper, tomato, potato, and petunia (red and yellow arrow respectively denotes cleavage sites) that has a strong target score, and may be a conserved mechanism for triggering DCL2 *PHAS* locus production in these species (B).

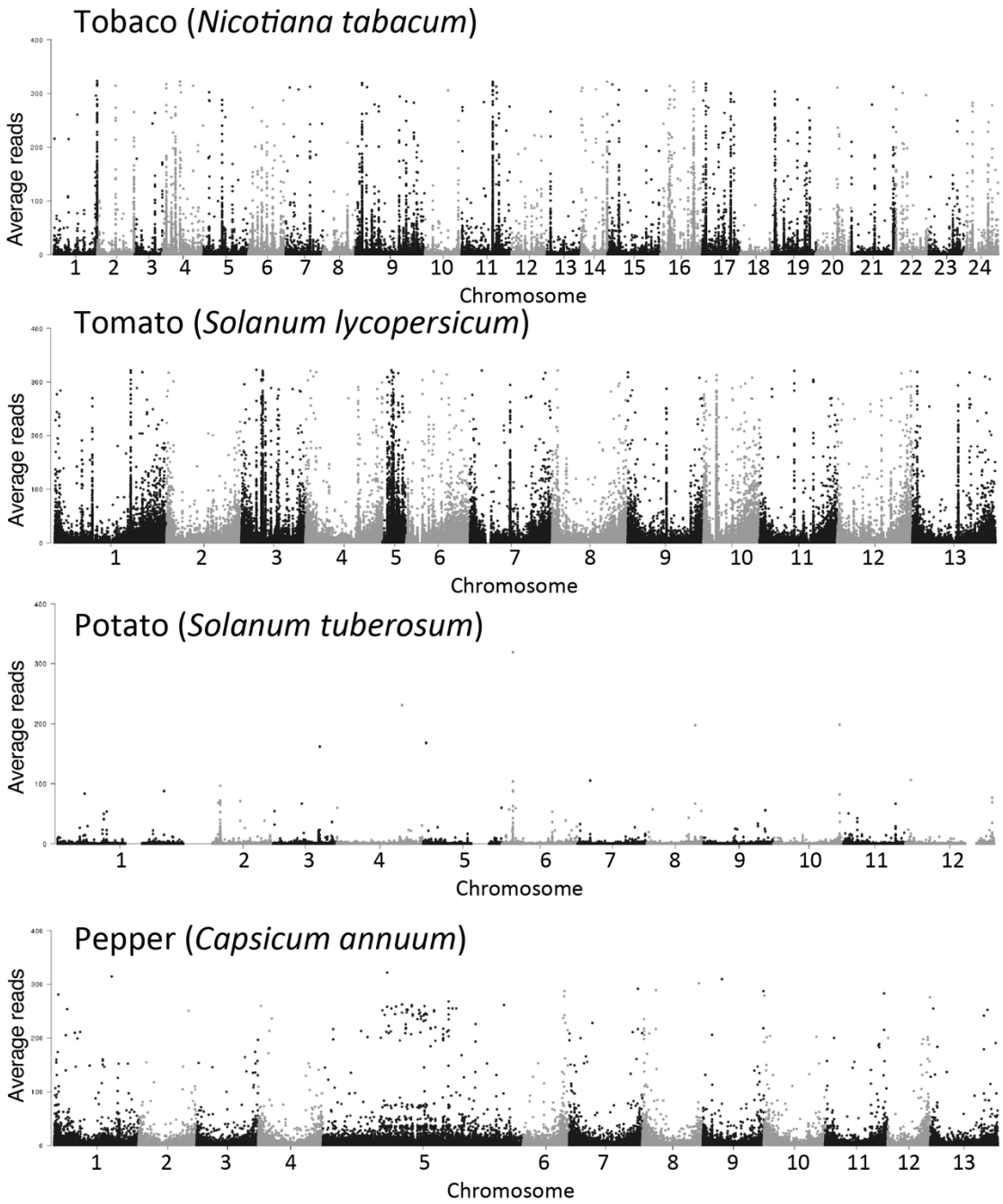

Figure 7: hc-siRNA expression across chromosomes in Solanaceae. Normalized read counts for 24-nt TE-associated hc-siRNAs are plotted across the assembled chromosomes for tobacco, tomato, potato, and pepper. The x-axis represents the chromosome number, alternating between grey and black, and the y-axis represents the average number of reads at each chromosome position. The average read number was calculated based on the number of available libraries for each species. As expected, the majority of hc-siRNAs map to telomeric ends. Unexpectedly, potato accumulates a low proportion of 24-nt hc-siRNAs relative to total sRNAs.

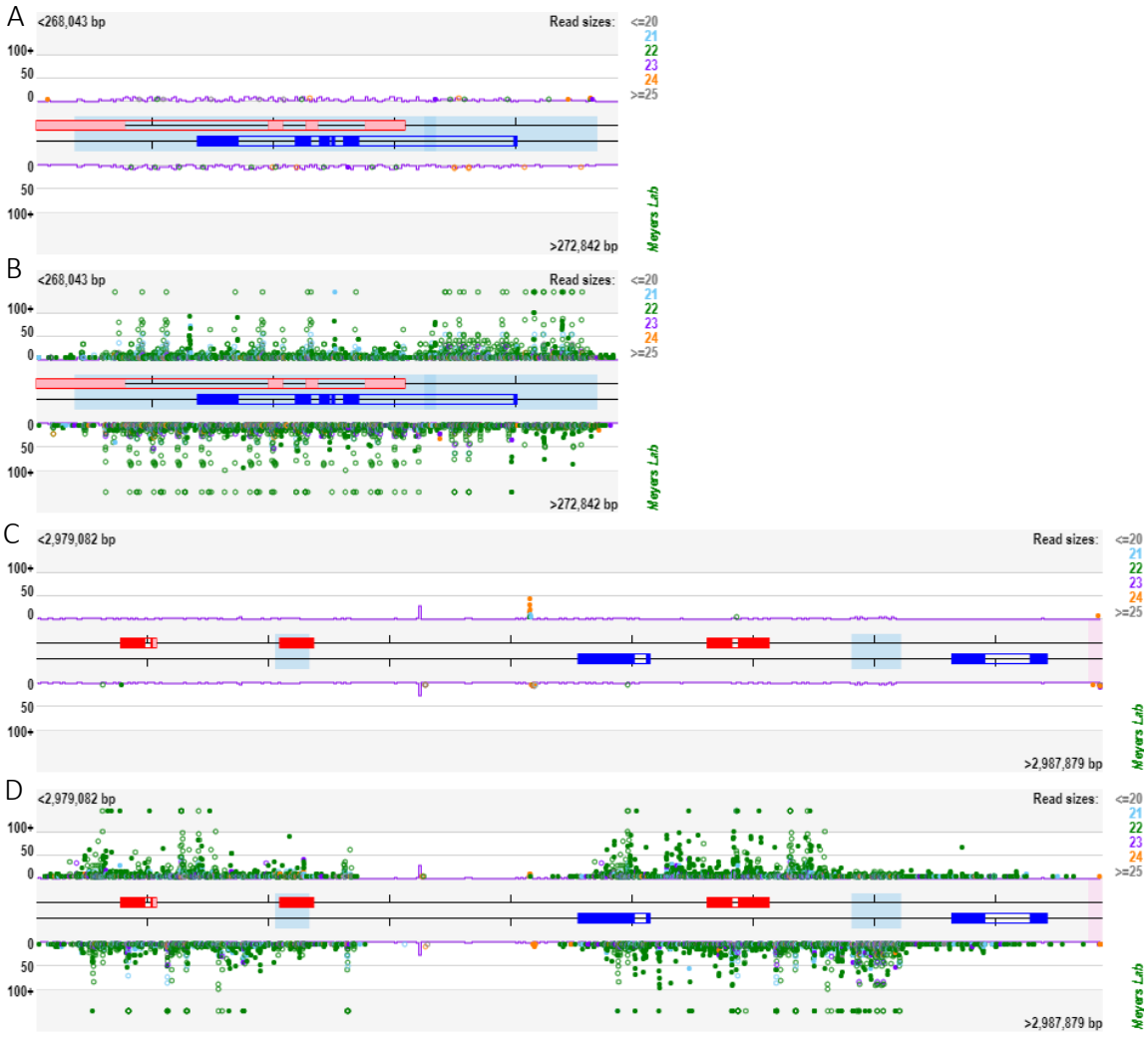

Figure 8: Tomato genome produces 22-nt sRNA clusters in response to geminivirus infection.
sRNA reads mapped to two genomic regions in an infected-control sample pair are shown. The central red and blue boxes represent gene models from the 3.0 version of *S. lycopersicum* genome, and shaded boxes represent repetitive sequences. Dots represent sRNA reads, color-coded by length, mapped to the genomic region, with abundance represented by the position along the Y axis. Hollow dots are multi-mappers, and solid dots are unique-mappers. (A) and (C) are from a control, mock-infected sample (Sly_leaves_t1) and (B) and (D) are from the corresponding virus-infected sample (Sly_leaves_t2). (A) and (B) show the genomic region Ch05:268043..272842. (C) and (D) show the genomic region Ch05:2979082..2987879.

Parsed Citations

Ahmed I, Sarazin A, Bowler C, Colot V, Quesneville H (2011) Genome-wide evidence for local DNA methylation spreading from small RNA-targeted sequences in Arabidopsis. Nucleic Acids Res 39: 6919–6931
Google Scholar: Author Only Title Only Author and Title

Altschul SF, Gish W, Miller W, Myers EW, Lipman DJ (1990) Basic local alignment search tool. J Mol Biol 215: 403–410
Google Scholar: Author Only Title Only Author and Title

Axtell MJ (2018) The small RNAs of Physcomitrella patens : Expression, function and evolution. Annual Plant Reviews online 113–142
Google Scholar: Author Only Title Only Author and Title

Axtell MJ (2013) ShortStack: comprehensive annotation and quantification of small RNA genes. RNA 19: 740–751
Google Scholar: Author Only Title Only Author and Title

Axtell MJ, Meyers BC (2018) Revisiting Criteria for Plant MicroRNA Annotation in the Era of Big Data. The Plant Cell 30: 272–284
Google Scholar: Author Only Title Only Author and Title

Axtell MJ, Snyder JA, Bartel DP (2007) Common functions for diverse small RNAs of land plants. Plant Cell 19: 1750–1769
Google Scholar: Author Only Title Only Author and Title

Axtell MJ, Westholm JO, Lai EC (2011) Vive la différence: biogenesis and evolution of microRNAs in plants and animals. Genome Biol 12: 221
Google Scholar: Author Only Title Only Author and Title

Bolger AM, Lohse M, Usadel B (2014) Trimmomatic: a flexible trimmer for Illumina sequence data. Bioinformatics 30: 2114–2120
Google Scholar: Author Only Title Only Author and Title

Bombarely A, Moser M, Amrad A, Bao M, Bapaume L, Barry CS, Bliek M, Boersma MR, Borghi L, Bruggmann R, et al (2016) Insight into the evolution of the Solanaceae from the parental genomes of Petunia hybrida. Nat Plants 2: 16074
Google Scholar: Author Only Title Only Author and Title

Bombarely A, Rosli HG, Vrebalov J, Moffett P, Mueller LA, Martin GB (2012) A draft genome sequence of Nicotiana benthamiana to enhance molecular plant-microbe biology research. Mol Plant Microbe Interact 25: 1523–1530
Google Scholar: Author Only Title Only Author and Title

Canto-Pastor A, Santos BA, Valli AA, Summers W, Schornack S, Baulcombe DC Enhanced resistance to bacterial and oomycete pathogens by short tandem target mimic RNAs in tomato. doi: 10.1101/396564
Google Scholar: Author Only Title Only Author and Title

Capella-Gutierrez S, Silla-Martinez JM, Gabaldon T (2009). trimAl: a tool for automated alignment trimming in large-scale phylogenetic analyses. Bioinformatics 25:1972-1973.
Google Scholar: Author Only Title Only Author and Title

Cardoso TC de S, Alves TC, Caneschi CM, Santana DDRG, Fernandes-Brum CN, Reis GLD, Daude MM, Ribeiro THC, Gómez MMD, Lima AA, et al (2018) New insights into tomato microRNAs. Sci Rep 8: 16069
Google Scholar: Author Only Title Only Author and Title

Chapman MA (2019) Introduction: The Importance of Eggplant. In MA Chapman, ed, The Eggplant Genome. Springer International Publishing, Cham, pp 1–10
Google Scholar: Author Only Title Only Author and Title

Chen C, Chen H, He Y, Xia R (2018a) TBtools, a Toolkit for Biologists integrating various biological data handling tools with a user-friendly interface. bioRxiv 289660
Google Scholar: Author Only Title Only Author and Title

Chen C, Zeng Z, Liu Z, Xia R (2018b) Small RNAs, emerging regulators critical for the development of horticultural traits. Horticulture Research 5: 6–8
Google Scholar: Author Only Title Only Author and Title

Chen H-M, Chen L-T, Patel K, Li Y-H, Baulcombe DC, Wu S-H (2010) 22-Nucleotide RNAs trigger secondary siRNA biogenesis in plants. Proc Natl Acad Sci U S A 107: 15269–15274
Google Scholar: Author Only Title Only Author and Title

Cosentino S, Iwasaki W (2018). SonicParanoid: fast, accurate and easy orthology inference. Bioinformatics. 35(1):149-51.
Google Scholar: Author Only Title Only Author and Title

Cuperus JT, Carbonell A, Fahlgren N, Garcia-Ruiz H, Burke RT, Takeda A, Sullivan CM, Gilbert SD, Montgomery TA, Carrington JC (2010) Unique functionality of 22-nt miRNAs in triggering RDR6-dependent siRNA biogenesis from target transcripts in Arabidopsis. Nat Struct Mol Biol 17: 997–1003
Google Scholar: Author Only Title Only Author and Title

Daxinger L, Kanno T, Bucher E, van der Winden J, Naumann U, Matzke AJM, Matzke M (2009) A stepwise pathway for biogenesis of 24-

nt secondary siRNAs and spreading of DNA methylation. EMBO J 28: 48–57
Google Scholar: Author Only Title Only Author and Title

Deng K, Yin H, Xiong F, Feng L, Dong P, Ren M (2021) Genome-wide miRNA expression profiling in potato (Solanum tuberosum L.) reveals TOR-dependent post-transcriptional gene regulatory networks in diverse metabolic pathway. PeerJ 9: e10704
Google Scholar: Author Only Title Only Author and Title

Edgar RC (2004) MUSCLE: Multiple sequence alignment with high accur- acy and high throughput. Nucleic Acids Res 32: 1792–1797
Google Scholar: Author Only Title Only Author and Title

Emms DM, Kelly S (2015). OrthoFinder: solving fundamental biases in whole genome comparisons dramatically improves orthogroup inference accuracy. Genome biology 16: 157.
Google Scholar: Author Only Title Only Author and Title

Esposito S, Aversano R, D'Amelia V, Villano C, Alioto D, Mirouze M, Carputo D (2018) Dicer-like and RNA-dependent RNA polymerase gene family identification and annotation in the cultivated Solanum tuberosum and its wild relative S. commersonii. Planta 248: 729–743
Google Scholar: Author Only Title Only Author and Title

Fan P, Leong BJ, Last RL (2019) Tip of the trichome: evolution of acylsugar metabolic diversity in Solanaceae. Curr Opin Plant Biol 49: 8–16
Google Scholar: Author Only Title Only Author and Title

Fei Q, Xia R, Meyers BC (2013) Phased, Secondary, Small Interfering RNAs in Posttranscriptional Regulatory Networks. Plant Cell 25: 2400–2415
Google Scholar: Author Only Title Only Author and Title

Galindo-González L, Mhiri C, Deyholos MK, Grandbastien M-A (2017) LTR-retrotransposons in plants: Engines of evolution. Gene 626: 14–25
Google Scholar: Author Only Title Only Author and Title

Goodin MM, Zaitlin D, Naidu RA, Lommel SA (2015) Nicotiana benthamiana: Its History and Future as a Model for Plant–Pathogen Interactions. Molecular Plant-Microbe Interactions 2015: 28–39
Google Scholar: Author Only Title Only Author and Title

Gu M, Liu W, Meng Q, Zhang W, Chen A, Sun S, Xu G (2014) Identification of microRNAs in six solanaceous plants and their potential link with phosphate and mycorrhizal signaling. J Integr Plant Biol 56: 1164–1178
Google Scholar: Author Only Title Only Author and Title

Guo Q, Qu X, Jin W (2015) PhaseTank: genome-wide computational identification of phasiRNAs and their regulatory cascades. Bioinformatics 31: 284–286
Google Scholar: Author Only Title Only Author and Title

Hardigan MA, Crisovan E, Hamilton JP, Kim J, Laimbeer P, Leisner CP, Manrique-Carpintero NC, Newton L, Pham GM, Vaillancourt B, et al (2016) Genome Reduction Uncovers a Large Dispensable Genome and Adaptive Role for Copy Number Variation in Asexually Propagated Solanum tuberosum. Plant Cell 28: 388–405
Google Scholar: Author Only Title Only Author and Title

Hellsten U, Wright KM, Jenkins J, Shu S, Yuan Y, Wessler SR, Schmutz J, Willis JH, Rokhsar DS (2013) Fine-scale variation in meiotic recombination in Mimulus inferred from population shotgun sequencing. Proc Natl Acad Sci U S A 110: 19478–19482
Google Scholar: Author Only Title Only Author and Title

Kakrana A, Li P, Patel P, Hammond R, Anand D, Mathioni SM, Meyers BC (2017) PHASIS: A computational suite for de novo discovery and characterization of phased, siRNA-generating loci and their miRNA triggers. bioRxiv 158832
Google Scholar: Author Only Title Only Author and Title

Kalyaanamoorthy S, Minh BQ, Wong TK, von Haeseler A, Jermiin LS (2017). ModelFinder: fast model selection for accurate phylogenetic estimates. Nature methods. 14:587.
Google Scholar: Author Only Title Only Author and Title

Klee HJ, Giovannoni JJ (2011) Genetics and control of tomato fruit ripening and quality attributes. Annu Rev Genet 45: 41–59
Google Scholar: Author Only Title Only Author and Title

Koenig DP, Sinha NR (2007) Genetic Control of Leaf Shape. Encyclopedia of Life Sciences. doi: 10.1002/9780470015902.a0020101
Google Scholar: Author Only Title Only Author and Title

Kozomara A, Birgaoanu M, Griffiths-Jones S (2019) miRBase: from microRNA sequences to function. Nucleic Acids Res 47: D155–D162
Google Scholar: Author Only Title Only Author and Title

Kozomara A, Griffiths-Jones S (2014) miRBase: annotating high confidence microRNAs using deep sequencing data. Nucleic Acids Res 42: D68–73
Google Scholar: Author Only Title Only Author and Title

Kramerov DA, Vassetzky NS (2011) Origin and evolution of SINEs in eukaryotic genomes. Heredity 107: 487–495
Google Scholar: Author Only Title Only Author and Title

Kuang H, Padmanabhan C, Li F, Kamei A, Bhaskar PB, Ouyang S, Jiang J, Buell CR, Baker B (2009) Identification of miniature inverted-repeat transposable elements (MITEs) and biogenesis of their siRNAs in the Solanaceae: new functional implications for MITEs. Genome Res 19: 42–56
Google Scholar: Author Only Title Only Author and Title

Langmead B (2010) Aligning short sequencing reads with Bowtie. Curr Protoc Bioinformatics Chapter 11: Unit 11.7
Google Scholar: Author Only Title Only Author and Title

Lei J, Sun Y (2014) miR-PREFeR: an accurate, fast and easy-to-use plant miRNA prediction tool using small RNA-Seq data. Bioinformatics 30: 2837–2839
Google Scholar: Author Only Title Only Author and Title

Leong BJ, Lybrand DB, Lou Y-R, Fan P, Schilmiller AL, Last RL (2019) Evolution of metabolic novelty: A trichome-expressed invertase creates specialized metabolic diversity in wild tomato. Sci Adv 5: eaaw3754
Google Scholar: Author Only Title Only Author and Title

Letunic I, Bork P (2019) Interactive Tree Of Life (iTOL) v4: Recent updates and new developments. Nucleic Acids Res 47: W256–W259
Google Scholar: Author Only Title Only Author and Title

Liao Z, Hodén KP, Singh RK, Dixelius C (2020) Genome-wide identification of Argonautes in Solanaceae with emphasis on potato. Scientific Reports. doi: 10.1038/s41598-020-77593-y
Google Scholar: Author Only Title Only Author and Title

Li H, Deng Y, Wu T, Subramanian S, Yu O (2010) Misexpression of miR482, miR1512, and miR1515 increases soybean nodulation. Plant Physiol 153: 1759–1770
Google Scholar: Author Only Title Only Author and Title

Liu Y, Teng C, Xia R, Meyers BC (2020) Phased secondary small interfering RNAs (phasiRNAs) in plants: their biogenesis, genic sources, and roles in stress responses, development, and reproduction. Plant Cell
Google Scholar: Author Only Title Only Author and Title

Lunardon A, Johnson NR, Hagerott E, Phifer T (2020) Integrated annotations and analyses of small RNA–producing loci from 47 diverse plants. Genome
Google Scholar: Author Only Title Only Author and Title

Martinez CC, Li S, Woodhouse MR, Sugimoto K, Sinha NR (2020) Spatial transcriptional signatures define margin morphogenesis along the proximal-distal and medio-lateral axes in tomato (Solanum lycopersicum) leaves. Plant Cell. doi: 10.1093/plcell/koaa012
Google Scholar: Author Only Title Only Author and Title

Ma Z, Zhang X (2018) Actions of plant Argonautes: predictable or unpredictable? Curr Opin Plant Biol 45: 59–67

Minh BQ, Nguyen MA, von Haeseler A (2013). Ultrafast approximation for phylogenetic bootstrap. Molecular biology and evolution. 30:1188-95.
Google Scholar: Author Only Title Only Author and Title

Mohorianu I, Schwach F, Jing R, Lopez-Gomollon S, Moxon S, Szittya G, Sorefan K, Moulton V, Dalmay T (2011) Profiling of short RNAs during fleshy fruit development reveals stage-specific sRNAome expression patterns: Time course study of short RNAs during fruit development. Plant J 67: 232–246
Google Scholar: Author Only Title Only Author and Title

Mosher RA, Melnyk CW (2010) siRNAs and DNA methylation: seedy epigenetics. Trends in Plant Science 15: 204–210
Google Scholar: Author Only Title Only Author and Title

Mueller LA, Solow TH, Taylor N, Skwarecki B, Buels R, Binns J, Lin C, Wright MH, Ahrens R, Wang Y, et al (2005) The SOL Genomics Network: a comparative resource for Solanaceae biology and beyond. Plant Physiol 138: 1310–1317
Google Scholar: Author Only Title Only Author and Title

Nakano M, McCormick K, Demirci C, Demirci F, Gurazada SGR, Ramachandruni D, Dusia A, Rothhaupt JA, Meyers BC (2020) Next-Generation Sequence Databases: RNA and Genomic Informatics Resources for Plants. Plant Physiol 182: 136–146
Google Scholar: Author Only Title Only Author and Title

Nguyen LT, Schmidt HA, Von Haeseler A, Minh BQ (2015). IQ-TREE: a fast and effective stochastic algorithm for estimating maximum-likelihood phylogenies. Molecular biology and evolution. 32:268-74.
Google Scholar: Author Only Title Only Author and Title

Niederhuth CE, Bewick AJ, Ji L, Alabady MS, Kim KD, Li Q, Rohr NA, Rambani A, Burke JM, Udall JA, et al (2016) Widespread natural variation of DNA methylation within angiosperms. Genome Biol 17: 194
Google Scholar: Author Only Title Only Author and Title

Park M, Park J, Kim S, Kwon J-K, Park HM, Bae IH, Yang T-J, Lee Y-H, Kang B-C, Choi D (2012) Evolution of the large genome in Capsicum annuum occurred through accumulation of single-type long terminal repeat retrotransposons and their derivatives. Plant J 69: 1018–1029
Google Scholar: Author Only Title Only Author and Title

Pokhrel, S., Huang, K., & Meyers, B. C. (2021). Conserved and non-conserved triggers of 24-nt reproductive phasiRNAs in eudicots. BioRxiv, https://doi.org/10.1101/2021.01.20.427321
Google Scholar: Author Only Title Only Author and Title

Pokhrel, S., Huang, K., Bélanger, S., Caplan, J. L., Kramer, E. M., & Meyers, B. C. (2020). Pre-meiotic, 21-nucleotide Reproductive PhasiRNAs Emerged in Seed Plants and Diversified in Flowering Plants. BioRxiv. https://doi.org/10.1101/2020.10.16.341925
Google Scholar: Author Only Title Only Author and Title

Pombo MA, Rosli HG, Fernandez-Pozo N, Bombarely A (2020) Nicotiana benthamiana, A Popular Model for Genome Evolution and Plant–Pathogen Interactions. The Tobacco Plant Genome 231–247
Google Scholar: Author Only Title Only Author and Title

Potato Genome Sequencing Consortium, Xu X, Pan S, Cheng S, Zhang B, Mu D, Ni P, Zhang G, Yang S, Li R, et al (2011) Genome sequence and analysis of the tuber crop potato. Nature 475: 189–195
Google Scholar: Author Only Title Only Author and Title

Qin C, Yu C, Shen Y, Fang X, Chen L, Min J, Cheng J, Zhao S, Xu M, Luo Y, et al (2014) Whole-genome sequencing of cultivated and wild peppers provides insights into Capsicum domestication and specialization. Proc Natl Acad Sci U S A 111: 5135–5140
Google Scholar: Author Only Title Only Author and Title

Särkinen T, Bohs L, Olmstead RG, Knapp S (2013) A phylogenetic framework for evolutionary study of the nightshades (Solanaceae): a dated 1000-tip tree. BMC Evol Biol 13: 214
Google Scholar: Author Only Title Only Author and Title

Schoft VK, Chumak N, Mosiolek M, Slusarz L, Komnenovic V, Brownfield L, Twell D, Kakutani T, Tamaru H (2009) Induction of RNA-directed DNA methylation upon decondensation of constitutive heterochromatin. EMBO Rep 10: 1015–1021
Google Scholar: Author Only Title Only Author and Title

Seo E, Kim T, Park JH, Yeom S-I, Kim S, Seo M-K, Shin C, Choi D (2018) Genome-wide comparative analysis in Solanaceous species reveals evolution of microRNAs targeting defense genes in Capsicum spp. DNA Res 25: 561–575
Google Scholar: Author Only Title Only Author and Title

Shinozaki Y, Nicolas P, Fernandez-Pozo N, Ma Q, Evanich DJ, Shi Y, Xu Y, Zheng Y, Snyder SI, Martin LBB, et al (2018) High-resolution spatiotemporal transcriptome mapping of tomato fruit development and ripening. Nature Communications. doi: 10.1038/s41467-017-02782-9
Google Scholar: Author Only Title Only Author and Title

Shivaprasad PV, Chen H-M, Patel K, Bond DM, Bruno A C, Baulcombe DC (2012) A MicroRNA Superfamily Regulates Nucleotide Binding Site–Leucine-Rich Repeats and Other mRNAs. Plant Cell 24: 859–874
Google Scholar: Author Only Title Only Author and Title

Slotkin RK, Vaughn M, Borges F, Tanurdzić M, Becker JD, Feijó JA, Martienssen RA (2009) Epigenetic reprogramming and small RNA silencing of transposable elements in pollen. Cell 136: 461–472
Google Scholar: Author Only Title Only Author and Title

Song Q-X, Liu Y-F, Hu X-Y, Zhang W-K, Ma B, Chen S-Y, Zhang J-S (2011) Identification of miRNAs and their target genes in developing soybean seeds by deep sequencing. BMC Plant Biol 11: 5
Google Scholar: Author Only Title Only Author and Title

Sun W, Xiang X, Zhai L, Zhang D, Cao Z, Liu L, Zhang Z (2018) AGO18b negatively regulates determinacy of spikelet meristems on the tassel central spike in maize. J Integr Plant Biol 60: 65–78
Google Scholar: Author Only Title Only Author and Title

Sun X, Zhang J, Li A, Yuan X (2013) mirPD: A pattern-based approach for identifying microRNAs from deep sequencing data. Digital Signal Processing 23: 1887–1896
Google Scholar: Author Only Title Only Author and Title

Taller D, Bálint J, Gyula P, Nagy T, Barta E, Baksa I, Szittya G, Taller J, Havelda Z (2018) Correction: Expansion of Capsicum annum fruit is linked to dynamic tissue-specific differential expression of miRNA and siRNA profiles. PLoS One 13: e0203582
Google Scholar: Author Only Title Only Author and Title

Tomato Genome Consortium (2012) The tomato genome sequence provides insights into fleshy fruit evolution. Nature 485: 635–641
Google Scholar: Author Only Title Only Author and Title

Turner SD (2014) qqman: an R package for visualizing GWAS results using Q-Q and manhattan plots. bioRxiv 005165
Google Scholar: Author Only Title Only Author and Title

Vaucheret H, Vazquez F, Crété P, Bartel DP (2004) The action of ARGONAUTE1 in the miRNA pathway and its regulation by the miRNA pathway are crucial for plant development. Genes Dev 18: 1187–1197
Google Scholar: Author Only Title Only Author and Title

Verhoeven KJF, Preite V (2014) Epigenetic variation in asexually reproducing organisms. Evolution 68: 644–655
Google Scholar: Author Only Title Only Author and Title

Vicient CM, Casacuberta JM (2017) Impact of transposable elements on polyploid plant genomes. Ann Bot 120: 195–207
Google Scholar: Author Only Title Only Author and Title

Vrbsky J, Akimcheva S, Watson JM, Turner TL, Daxinger L, Vyskot B, Aufsatz W, Riha K (2010) siRNA-mediated methylation of Arabidopsis telomeres. PLoS Genet 6: e1000986
Google Scholar: Author Only Title Only Author and Title

de Vries S, Kloesges T, Rose LE (2015) Evolutionarily Dynamic, but Robust, Targeting of Resistance Genes by the miR482/2118 Gene Family in the Solanaceae. Genome Biol Evol 7: 3307–3321
Google Scholar: Author Only Title Only Author and Title

Waese J, Fan J, Pasha A, Yu H, Fucile G, Shi R, Cumming M, Kelley L, Sternberg M, Krishnakumar V, Ferlanti E, Miller J, Town C, Stuerzlinger W, Provart NJ (2017). ePlant: Visualizing and Exploring Multiple Levels of Data for Hypothesis Generation in Plant Biology. Plant Cell 29:1806-1821.
Google Scholar: Author Only Title Only Author and Title

Wang X, Weigel D, Smith LM (2013) Transposon variants and their effects on gene expression in Arabidopsis. PLoS Genet 9: e1003255
Google Scholar: Author Only Title Only Author and Title

Wang Z, Hardcastle TJ, Pastor AC, Yip WH, Tang S, Baulcombe DC (2018) A novel DCL2-dependent miRNA pathway in tomato affects susceptibility to RNA viruses. Genes & Development 32: 1155–1160
Google Scholar: Author Only Title Only Author and Title

Won SY, Yumul RE, Chen X (2014) Small RNAs in Plants. In SH Howell, ed, Molecular Biology. Springer New York, New York, NY, pp 95–127
Google Scholar: Author Only Title Only Author and Title

Wu, H., Li, B., Iwakawa, H. oki, Pan, Y., Tang, X., Ling-hu, Q., Liu, Y., Sheng, S., Feng, L., Zhang, H., Zhang, X., Tang, Z., Xia, X., Zhai, J., & Guo, H. (2020). Plant 22-nt siRNAs mediate translational repression and stress adaptation. Nature 581: 81-93
Google Scholar: Author Only Title Only Author and Title

Wu L, Zhang Q, Zhou H, Ni F, Wu X, Qi Y (2009) Rice MicroRNA Effector Complexes and Targets. The Plant Cell 21: 3421–3435
Google Scholar: Author Only Title Only Author and Title

Xia R, Meyers BC, Liu Z, Beers EP, Ye S, Liu Z (2013) MicroRNA superfamilies descended from miR390 and their roles in secondary small interfering RNA Biogenesis in Eudicots. Plant Cell 25: 1555–1572
Google Scholar: Author Only Title Only Author and Title

Xia R, Xu J, Arikit S, Meyers BC (2015) Extensive Families of miRNAs and PHAS Loci in Norway Spruce Demonstrate the Origins of Complex phasiRNA Networks in Seed Plants. Mol Biol Evol 32: 2905–2918
Google Scholar: Author Only Title Only Author and Title

Xie Z, Kasschau KD, Carrington JC (2003) Negative feedback regulation of Dicer-Like1 in Arabidopsis by microRNA-guided mRNA degradation. Curr Biol 13: 784–789
Google Scholar: Author Only Title Only Author and Title

Zhai J, Jeong D-H, De Paoli E, Park S, Rosen BD, Li Y, González AJ, Yan Z, Kitto SL, Grusak MA, et al (2011) MicroRNAs as master regulators of the plant NB-LRR defense gene family via the production of phased, trans-acting siRNAs. Genes Dev 25: 2540–2553
Google Scholar: Author Only Title Only Author and Title

Zhang H, Xia R, Meyers BC, Walbot V (2015) Evolution, functions, and mysteries of plant ARGONAUTE proteins. Curr Opin Plant Biol 27: 84–90
Google Scholar: Author Only Title Only Author and Title

Zhang R, Marshall D, Bryan GJ, Hornyik C (2013) Identification and characterization of miRNA transcriptome in potato by high-throughput sequencing. PLoS One 8: e57233
Google Scholar: Author Only Title Only Author and Title

Zuo J, Grierson D, Courtney LT, Wang Y, Gao L, Zhao X, Zhu B, Luo Y, Wang Q, Giovannoni JJ (2020) Relationships between genome methylation, levels of non-coding RNAs, mRNAs and metabolites in ripening tomato fruit. Plant J 103: 980–994
Google Scholar: Author Only Title Only Author and Title